Ray entity based post processing of ray tracing data for continuous modeling of radio channel

Nikola Mataga, Micro-link, Jaruščica 9a, Zagreb, Croatia

Radovan Zentner, University of Zagreb, Faculty of Electrical Engineering and Computing, Unska 3, Zagreb, Croatia

Ana Katalinić Mucalo, Croatian Post and Electronic Communications Agency, Ulica Roberta Frangeša Mihanovića 9, Zagreb, Croatia

Corresponding author: Radovan Zentner, University of Zagreb, Faculty of Electrical Engineering and Computing, Unska 3, 10000 Zagreb, Croatia, *radovan.zentner@fer.hr*

Key Points

1. Ray tracing data consists of variables such as angles of arrival and departure, ray length, received power and polarity.
2. Using ray tracing is challenging because of the time-consuming simulations, predefined resolution of calculated location points and huge demand on storage capacity.
3. This paper provides ray entity based interpolation technique that reduces memory and processor time demand and yet gives more detailed description of the radio environment.

***Abstract*— Ray tracing data is usually given as a vector of many variables, such as angles of arrival and departure, transmitter and receiver coordinates, ray length and delay, received power level, and polarity. Usually, these values are given in raw data with some resolution that covers the area of interest where the**

simulation is performed. There are two main drawbacks of such approach; firstly a huge amount of storage capacity is typically needed to store all necessary data and secondly, although the area of interest is covered by a certain resolution, it is not straightforward, but rather nearly impossible to interpolate between sample points and new time and memory consuming simulations are necessary in order to increase the resolution of simulations. This paper addresses the two mentioned drawbacks of ray tracing, suggesting a procedure based on the concept of ray entities to both enable continuous interpolation of ray tracing data and reduce memory needed for storing data. Ray entity is a set of rays that all undergo the same series of propagation phenomena (direct ray, diffraction, reflection or scattering) on the same objects (building walls or edges). The method is given and illustrated for reflection and diffraction phenomena and diffuse scattering was not included, but discussion is easily extended to this propagation type as well. The paper gives detailed statistics of entities' length and rays' count per simulated receiver point in few illustrative examples and provides an insight into how to interpolate angles of arrival and departure, ray length and received power level in order to provide continuous description of the radio environment.

Keywords: radio channel modeling, geometry-based stochastic channel models (GBSCM), visibility regions, ray entity, urban model, ray-tracing interpolation

1. INTRODUCTION

The importance of reference channel models (RCM) as a distinct kind of radio channel modeling has already been widely realized [P. Almers et al., 2007]. RCM's purpose is to adequately simulate typical radio environment properties, and thus be used as a test platform for the development of new generations of access radios, exploring modulation and coding techniques, different smart antenna and MIMO system designs etc. Most of commonly used RCMs are stochastic, or more precisely, geometry-based stochastic channel models (GBSCM). This means that GBSCM parameters are generated from some stochastic process [P. Almers et al., 2007; K. Haneda, 2011]. Therefore, these models suffer the risk of unrealistic channel realizations due to their random nature, and of inaccuracies of the parameterization extraction approximation.

Current GBSCMs are mostly measurement-based, so prior to parameterization data from real world measurements are needed. Besides the fact that measurements are time consuming and expensive, additional limitations are caused by antenna properties, phase synchronization, measurement errors and random events that could be present only while specific measurement is taking place and especially if measurements have not been repeated on the same route or measurement set which is shown in earlier studies [Molisch et al., 2006; H. Asplund et al., 2006; L. M. Correia (Ed.), 2006; I. Sirkova, 2006].

Deterministic RCMs are suggested as a possibility in earlier paper [A. Katalinić Mucalo et al. 2012], but they are still not explored enough as an achievable option for RCMs, mainly due to their complexity and vast system requirements. The feasible alternative for feeding geometry-based deterministic RCM would be a set of ray tracing (RT) simulated environments. Ray tracing allows high-resolution simulations, thus providing a very detailed description of the radio environment and the propagation phenomena. However, RT is a very time-consuming process with extremely high demands for both CPU time and memory capacities, in order to store and manipulate all the data necessary for a very fine spatial resolution. Also, RT computational burden grows significantly with the number of considered receiver points. In this paper it is elaborated how to decrease stored RT data and enable interpolation of omitted receiver points while ensuring even higher resolution then the ones originally sampled. These at first hand contradictive aims are achieved by smart interpolation process using ray entity concept that in the end decreases needed computational time and complexity, while preserving the accuracy of the full ray tracing model.

The paper analyzes the arrangement of the rays in an urban multipath environment and in particular virtual sources in cases of reflection and diffraction propagation with up to two interactions. Similar work on ray dynamics in multipath environment has already been done in [A. Katalinić, R. Zentner, 2011] and showed that due to the nature of diffraction there is no common stationary virtual source of neighboring rays even when ending very close (below 1 m) to each other and in spite of undergoing identical multipath interactions. In that work any considerable visibility length could be obtained only by approximation using tolerance - basically approximating VTx locus, which is part of a circle, by a point. The motivation for that was to obtain parameters for stochastic based reference channel models that incorporate stationary clusters, i.e. virtual sources, but no virtual sources that move in correlation with user movement. Further in paper ray entity definition will be given, and will be different from one in [A. Katalinić, R. Zentner, 2011].

Appreciating the finding that diffraction causes virtual source of rays to move in correlation to moving of receiver [R. Zentner et al., 2013] this paper analyzes a new method for detection of visibility area and virtual sources for moving receivers. The paper elaborates the method for determining trajectories of virtual sources and how those trajectories can be utilized for the interpolation of RT results. The paper is limited by taking into account only direct rays, and reflected and diffracted rays up to two interactions per ray. Although 3D RT tool [V. Degli-Esposti et al., 2004; F. Fuschini et al., 2008.] used for feeding the interpolation engine is calculating both diffuse scattering and over-the-roof (ORT) diffraction, in this paper these two propagation modes are not considered. However, the discussion and presented concepts are easily extensible to these propagation phenomena as well.

The paper is organized as follows. In Section II the concepts of reflection and diffraction propagation phenomena, ray entities and virtual sources will be shown as well as using those concepts for the interpolation of RT results. In Section III ray entity detection will be explained for three examples in an urban scenario and the statistics of ray entity lengths will be given. Section IV will discuss receiver and virtual sources trajectories that are needed so that interpolation of ray length, angles and power can be interpolated for enhancing RT performance and as a building block of deterministic RCM. The paper ends with conclusions given in Section V.

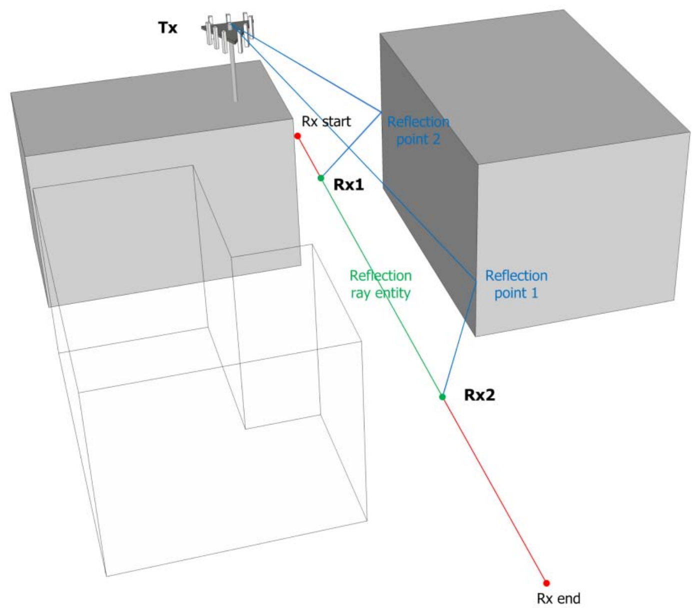

(a)

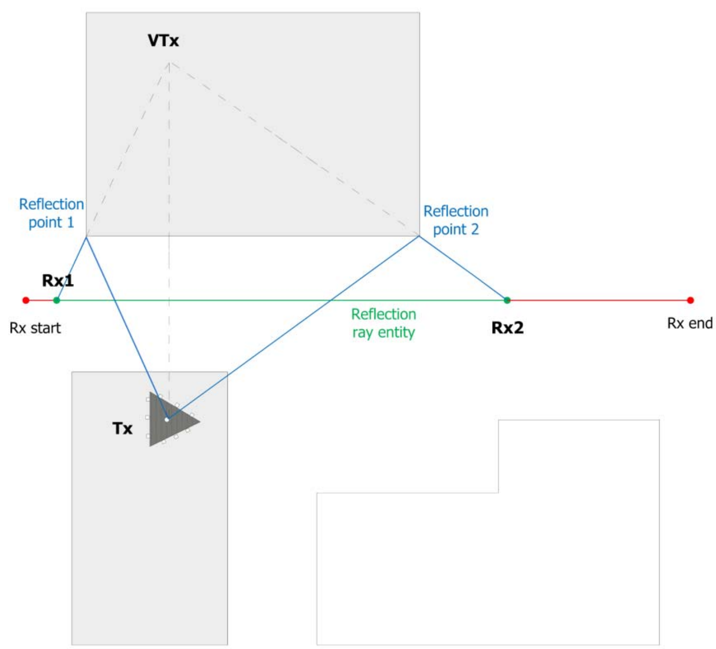

(b)

Fig. 1. 3D view (a) and top view (b) illustrating visibility of receiver route, reflection ray entity and location of virtual source

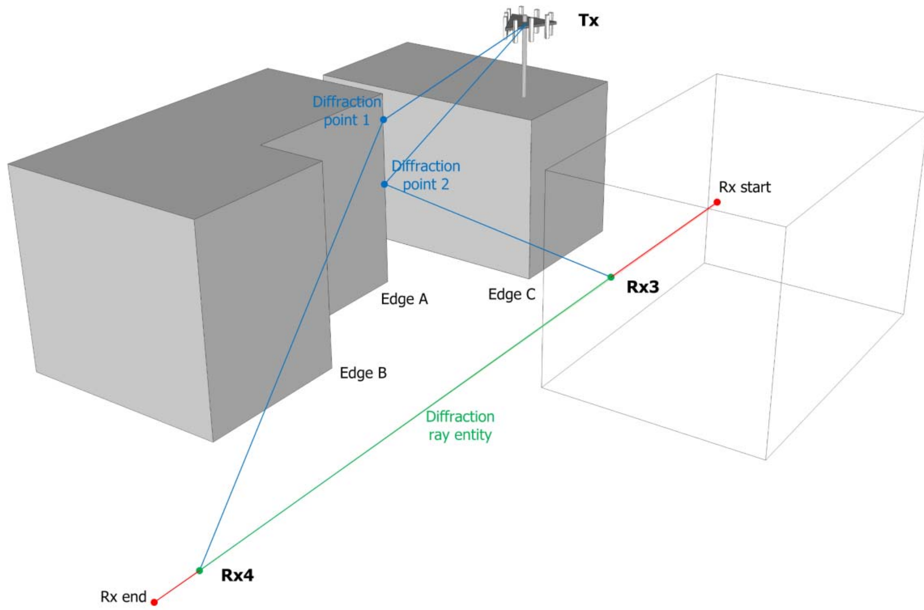

(a)

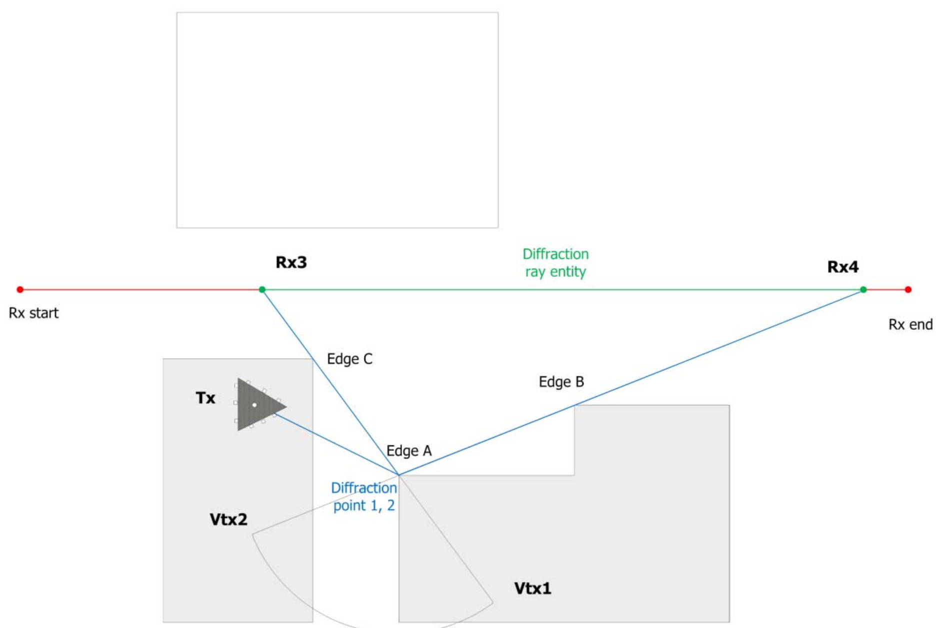

(b)

Fig. 2. 3D view (a) and top view (b) illustrating visibility of receiver route, diffraction ray entity and location of virtual sources

2. Ray Entities and Virtual Sources

Figures 1. and 2. give 3D and top view (ground plan) of a simple setting of one transmitter (Tx), three buildings, and a receiver route of interest. Fig 1. describes reflection points, virtual source and ray entity for reflection and Fig 2. describes the same for diffraction. In Fig. 1. rays reflected from building wall will, due to geometry reasons be present only at the portion of the receiver route (red line) from Rx1 to Rx2 (green line). The set of rays from Rx1 to Rx2 is called **ray entity** (RE) in which all rays undergo the same propagation phenomenon, here reflection from the building wall. Another property of this RE is that all rays arriving at the receivers come from the identical stationary virtual source, VTx_R.

Fig. 2. depicts a ray entity which occurs due to a single diffraction at the vertical edge A. Due to the shadowing from edges B and C, this ray entity is also present at the receiver route from point Rx3 to Rx4 (green line). Here, in case of diffraction, virtual transmitter is not a single point for the whole entity, but a section of a circle, from VTx1 to VTx2, and slides circularly as the receiver slides along the route section where entity rays are present. The diffracted ray incidence angle to the edge equals the Kellers kone semi-angle which is described in [J.B.Keller, 1962; D.A.McNamara et al., 1990].

Virtual source for diffraction from vertical edges is often considered to be the last interaction point on the building edge. However, looking from the receiver's perspective it is much more convenient to extend the ray with the same spatial angle in the direction of the interaction point on the edge for the length of the ray from that interaction point to the transmitter. Thus the locus of virtual sources for diffraction ray entity is not a line along the interaction edge but a section of a circle at the height of the transmitter and parallel to the ground as can be seen in Fig 2. Since VTx circle is defined with any three points it is possible to interpolate any virtual source and from calculated VTx to obtain ray properties for any receiver point along the route by extending the ray through building edge to the route with straight line. Thus, rays at the receiver points along the receiver route that were not previously simulated using RT, can be easily calculated using existing Tx coordinates, edge coordinates, initial ray length and VTx circle virtually at no computational cost. For pure reflections there is no need for interpolation of virtual source, since the virtual source is stationary for this kind of propagation as can be seen on Fig. 1. For multiple interactions i.e. double diffraction, reflection with diffraction and diffraction with reflection the situation is a bit more complex. Fig. 3. shows double diffraction in 2D and 3D where it can be seen that moving receiver changes only the length $\overline{AR_x}$ and angle $\angle T_x R_x E$ so virtual sources for double diffraction are also sections of circles that can be easily calculated by extending the ray with the same elevation angle from Rx through point B to Tx i.e. the triangle RxETx can be unfolded as depicted in Fig. 3.b. It should be noted that in Fig. 3. Rx route and all three buildings have the same ground level. However, even when elevation of point E is different from elevation of point Rx, the triangle stays the same, only the vertical cathetus length is now $h_{Tx} + \Delta h$ where Δh is difference in ground level heights between receiver and Tx. For events where the first interaction is diffraction and the second interaction reflection if we mirror the receiver route in relation to the reflecting wall the interpolation is simplified to the one diffraction case. For events where the first interaction is reflection and the second interaction diffraction if we mirror the transmitter in relation to the reflecting wall the interpolation is again simplified to the one diffraction case.

Detection of ray entities is rather simple. For each ray obtained by RT a signature is assigned, that contains sub-signatures of identity of first and second interaction objects (edges, surfaces) at which the ray lands, and the types of interactions (diffraction, reflection) that ray undergoes there. Then all rays with same signatures and neighboring each other at Rx side are grouped into same entity, and entity's minimal set of parameters for its description is recorded. List of these parameters will be given at the end of the paper in discussion about memory requirements for storing entities.

Virtue of ray entity concept is that a number of rays obtained by ray tracing and belonging to the same ray entity can be stored as one ray entity, and it will be shown how thus memory for storing ray tracing data can be spared.

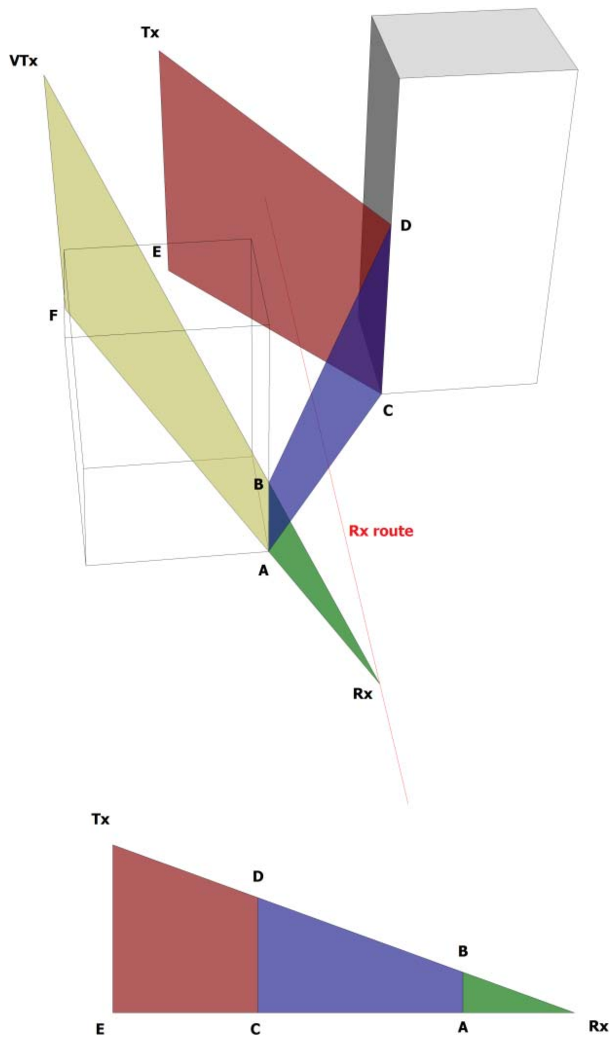

Fig. 3. 3D and top view illustrating unfolded triangle with Tx and Vtx for the ray undergoing double diffraction

Once the ray entities are detected and stored, not only the initial RT results at initially simulated discrete Rx points can be retrieved at small computational cost, but also the RT results on arbitrary locations between these discrete Rx points can be obtained by interpolation, under assumption that there exist only ray entities present at adjoining Rx points.

The ray entity record can also offer an estimate of sufficiency or insufficiency of initial Rx resolution, that comes from observing RT results without need for variation in resolution, by counting how many entities were formed only at a single Rx. This criterion will be applied on results in this paper and give resolution of 1m to be quite reasonable for considered environments.

It is worth noting also that unnecessarily high resolution of receivers during initial RT simulation would not increase memory need if data is stored as ray entities, whereas in conventional storing of all ray data memory space is roughly proportional to resolution increase.

Therefore ray entity concept offers users versatility according to their needs and computer capacity. Either they can carefully estimate when initial Rx resolution is sufficient, and then form ray entities for further use of data, or go using "brute force" by having very high initial Rx resolution and then form ray entities for further use. In both cases results would usually be similar, in former case sparing some initial computer power on expense of potentially missing some entities, and in later case using excessive computer power for reduced risk of missing some entities.

3. Detection of Ray Entities from RT Results

The analysis is performed on RT simulated radio environments where a mobile unit is slid incrementally along a receiver (Rx) route. All rays obtained from simulations are compared by their interaction points (walls or edges) and propagation modes (direct ray, reflection and diffraction) and then grouped into ray entities, consisting of rays which underwent same types of propagation effects, in the same order and on the same objects. Rays within the same RE form an entity visibility region, a section of a receiver route.

An example will be given using three RT simulations on a map of Stockholm (Fig. 4). The first simulation route is the shortest, a 39 m long straight route 1, the second simulation is 238m long L-shaped route 2 and the third simulation is 100m straight route 3. All three simulations have resolution of 1m, i.e.

Rx samples are taken every 1m. The propagation modes simulated were LOS, 1st and 2nd order reflection, 1st and 2nd order diffractions and mixed rays.

Table 1 presents properties of each route, i.e. overall number of rays, range and average of number of rays at a single Rx point. All rays regardless of power were included under "Raw data (no threshold)" section, but also same data after applying power threshold of 150 dBW was considered as well, under "Power threshold 150 dBW" section. The power threshold was set to -150dBW since most modern communication systems already have few orders of magnitude weaker receiver sensitivity even for simple modulations like QPSK (Quadrature Phase-Shift Keying).

For routes 1, 2 and 3 the power threshold reduced the total power at the receiver locations on average for negligible 0.0037 dB, 0.00048 dB and 0.0029 dB respectively, and maximal observed reduction at any one Rx for was for 0.0044 dB, 0.004 dB and 0.013 dB.

Raw data is interesting because imposing threshold may cut entity into two or several entities and data after imposed power threshold is interested since these data is more likely to be relevant in practice.

Table 1. Properties of considered routes

Route #	Raw data (no treshold)			Power threshold 150 dBW		
	# of rays (total)	# of rays at one Rx		# of rays (total)	# of rays at one Rx	
		range	average		range	average
1	2,060	36-107*	52.8	1,384	24-68	35.5
2	26,176	7-449	196.8	16,456	4-263	123.7
3	11,137	50-242	110.3	5,494	26-109	54.4

*few Rx locations with no rays at all

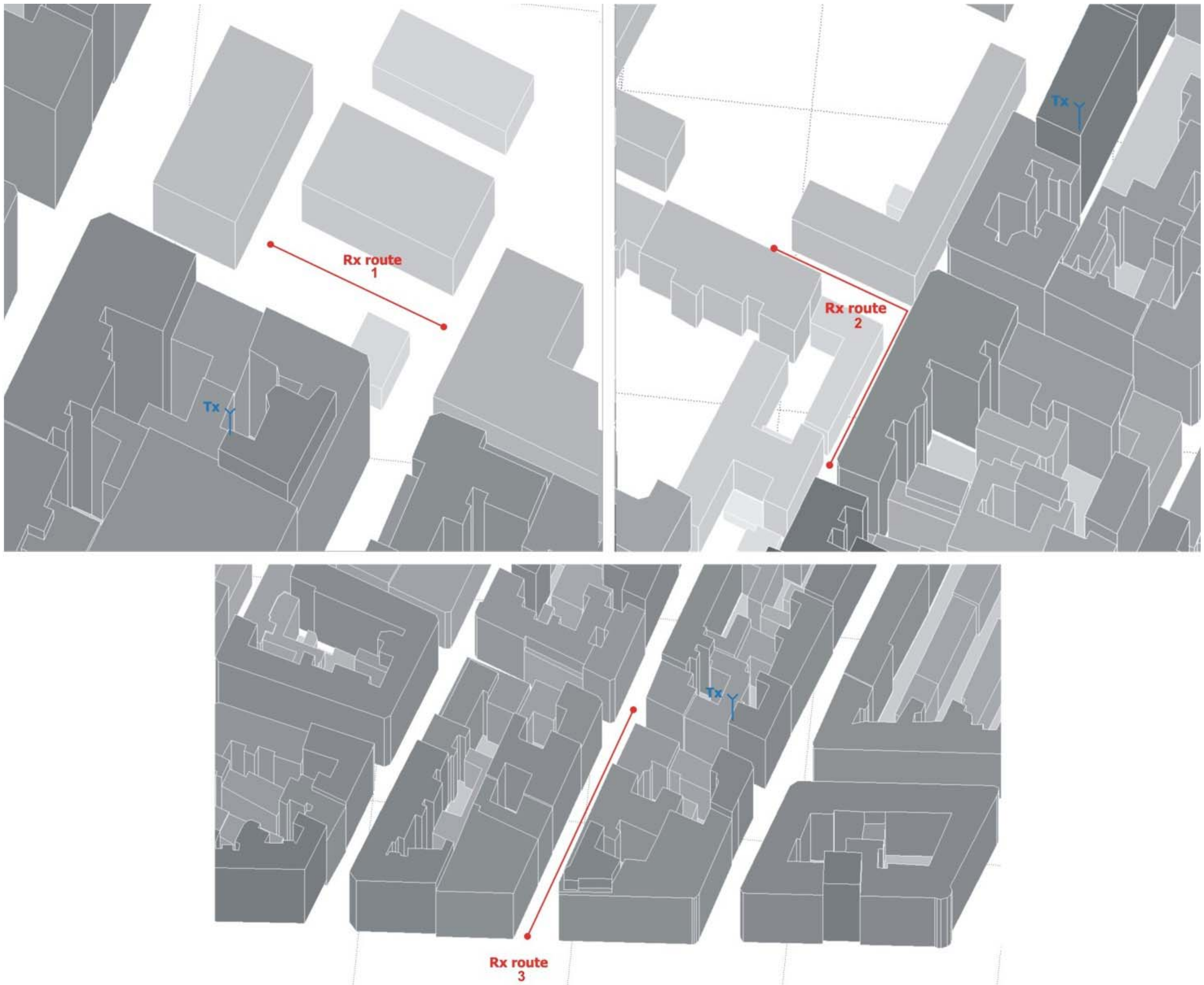

Fig. 4. Simulation scenarios: a 39m long straight route 1, 133m L-shaped route 2 and 100m straight route 3 in city of Stockholm

Fig. 5. shows distribution of entities detected along the straight route 1 by their length. It is given for a case with no power threshold on rays (Fig. 5.a) and with power threshold (Fig. 5.b). Observing Fig.5. one can see that significant portion of entities is of length 1, i.e. were detected only at on Rx point in RT simulations. This may suggest that Rx resolution of 1 is not sufficient and that many entities of shorter

duration would be lost. However, more fair estimation of single-point entities' contribution would not be from distribution of entities by their length, but rather from the distribution of rays by entity length, since shorter entities are less significant comparing to longest entities and distribution of rays by entity lengths will resemble this fact.

Fig. 6. shows the distribution of detected rays by entity length along the straight route 1 and it can be seen that portion of rays allocated to shortest entity is quite small. This fact suggests that it is in case of route 1 reasonable to conclude that Rx resolution of 1 meter was quite sufficient.

Regarding difference between data with and without power threshold, figures 5 and 6 show that expected proportionate difference in overall number of rays and entities is present, but there is no significant difference in distribution shape. Since for routes 2 and 3 also no significant difference in distribution shape was observed, for them only cases with power threshold will be presented.

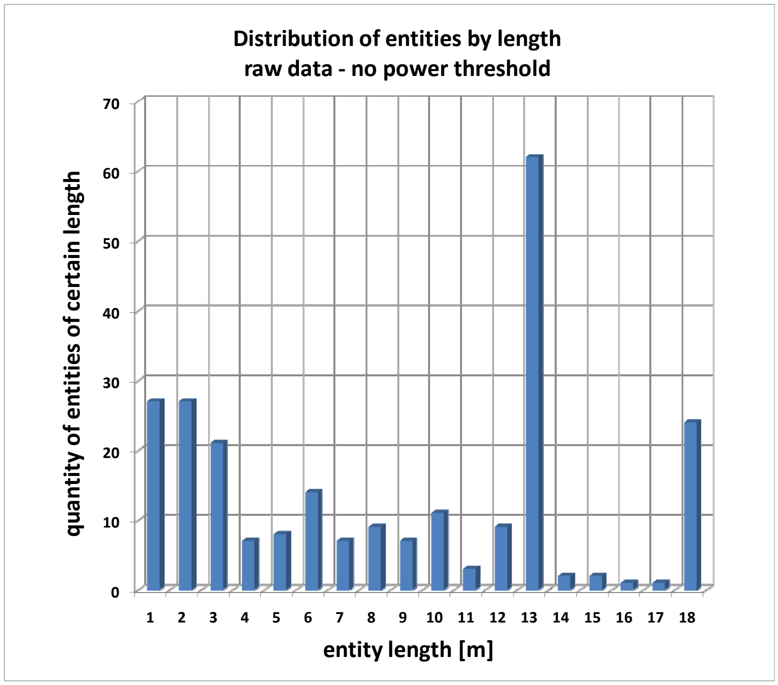

(a)

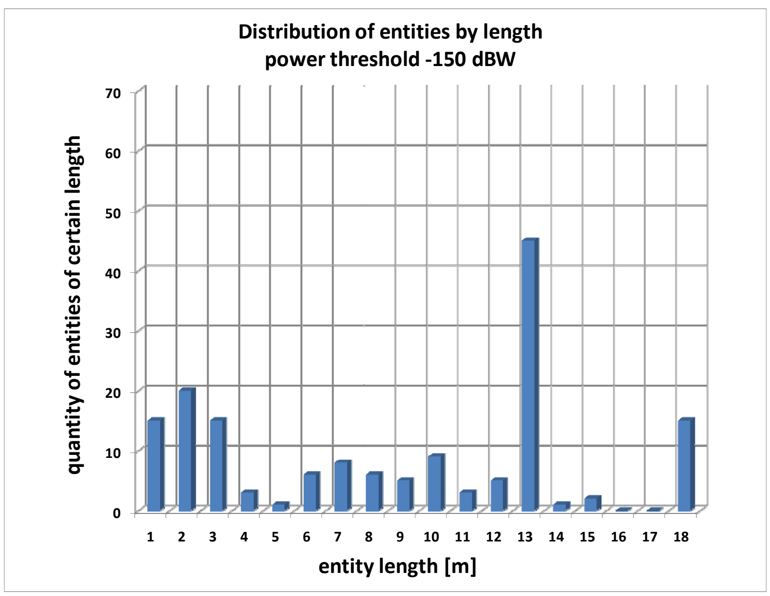

(b)

Fig. 5. Distribution of entities along the straight route 1 by length. It is given for raw ray data (a) and after applying power threshold of -150dBW (b).

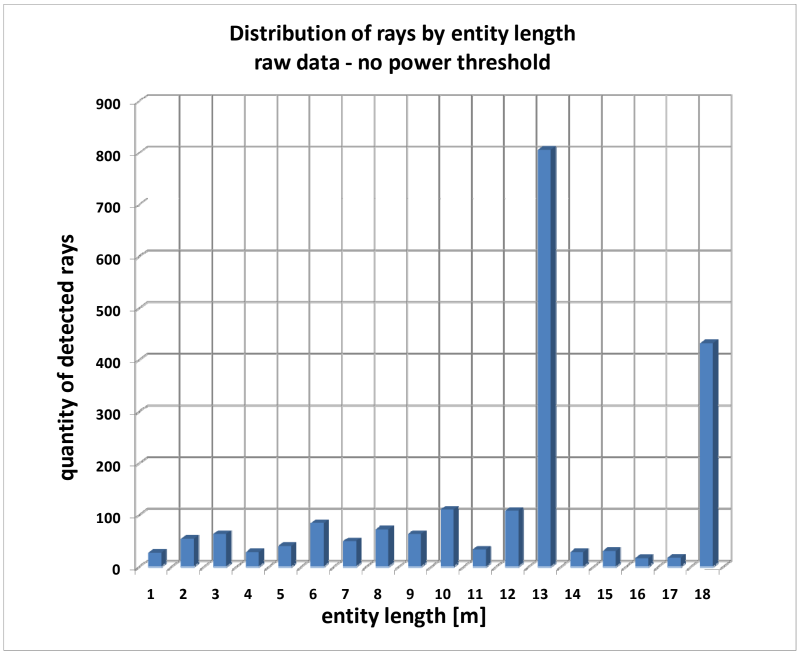

(a)

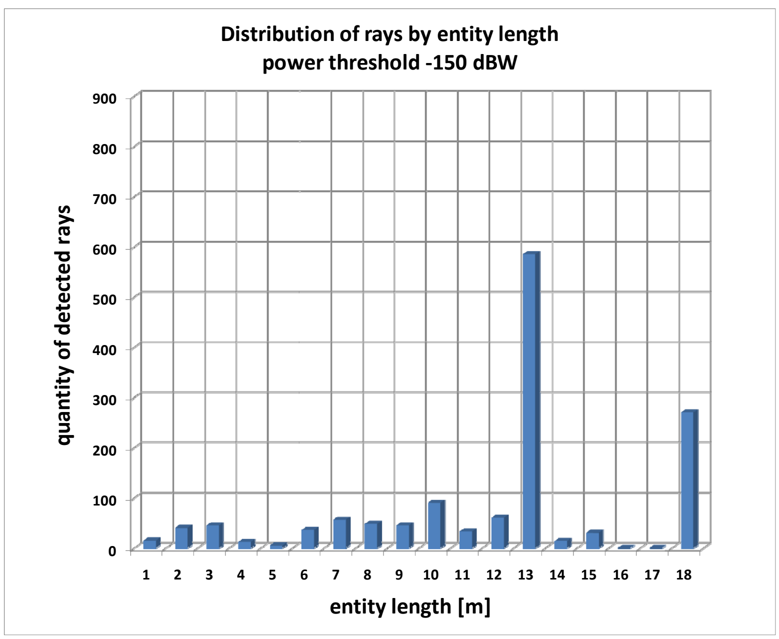

(b)

Fig. 6. Distribution of rays along the straight route 1 by entity length. It is given for raw ray data (a) and after applying power threshold of -150dBW (b).

Fig. 7. shows distribution of entities by length (a) and distribution of detected rays by entity length, along the L-shaped route 2, for case with -150dBW power threshold. Although fig. 7 (a) shows that portion of shortest, 1m long entities is largest, fig. 7 (b) clearly shows how negligible is amount of rays that form shortest entities, comparing to amount of all rays obtained in RT simulations.

The same can be said for route 3, presented in same way in fig. 8. Therefore for all routes considered it is quite certain that resolution for RT of 1m was sufficient.

Figures 5., 6., 7., and 8. show that numerous ray entities of considerable length are detected in considered example scenarios.

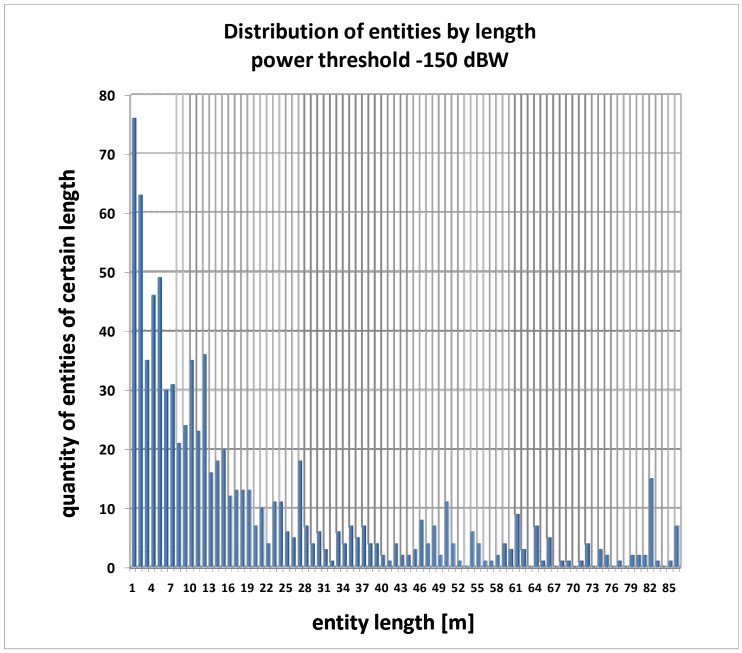

(a)

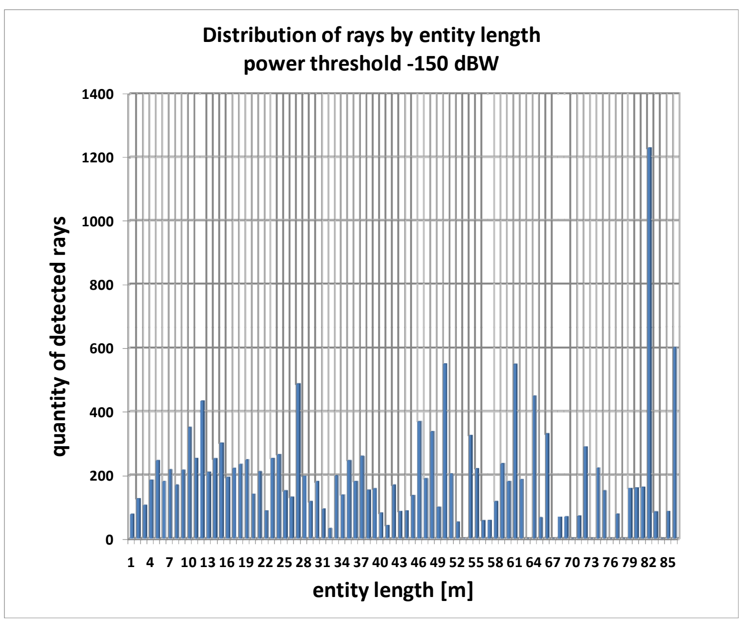

(b)

Fig. 7. Distribution of entities along the L shaped route 2 by length (a) and distribution of rays along the L shaped route 2 by entity length (b). They are given for applying power threshold of -150dBW.

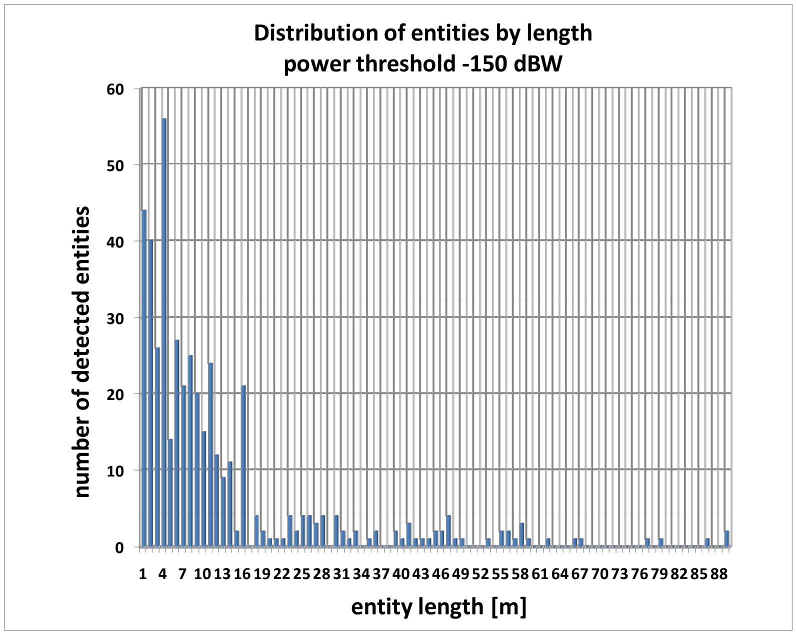

(a)

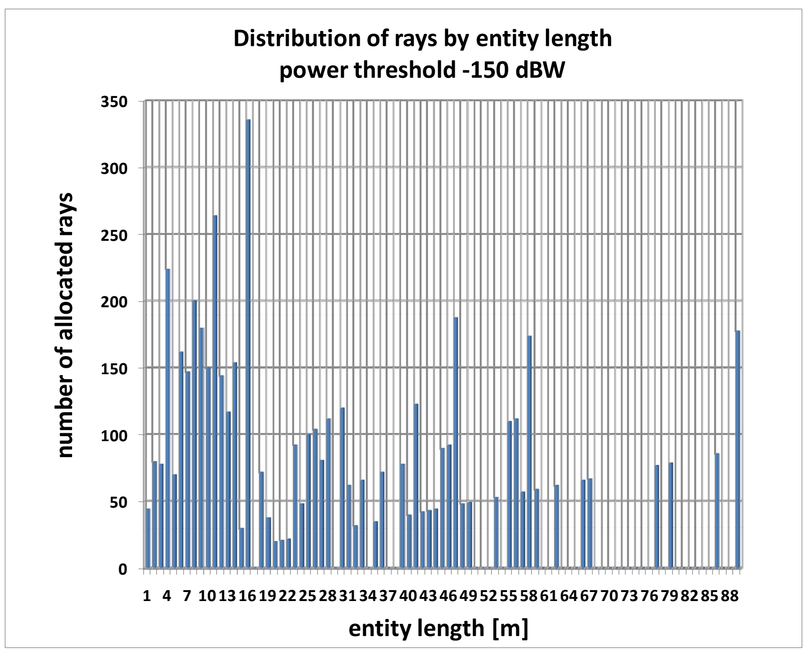

(b)

Fig. 8. Distribution of entities along the straight route 3 by length (a) and distribution of rays along the straight route 3 by entity length (b). They are given for applying power threshold of -150dBW.

4. Interpolation of RT results using Ray Entities

One entity from L-shaped route (route 2) with the visibility length of 86 m shall be used to illustrate typical relationship between the actual source, interaction points, entity visibility and virtual sources. Fig. 9. gives a ground plan of a scene in Fig. 4 (route 2), but with a limited number of elements, only those relevant for this entity: location of transmitter (red triangle), actual ray path (red), entity visibility range (green) and locus of virtual sources for the entity. Fig. 9 conveniently shows ray entity that is present along one street of L-shaped route and then disappears shortly after the receiver enters the other street of the route.

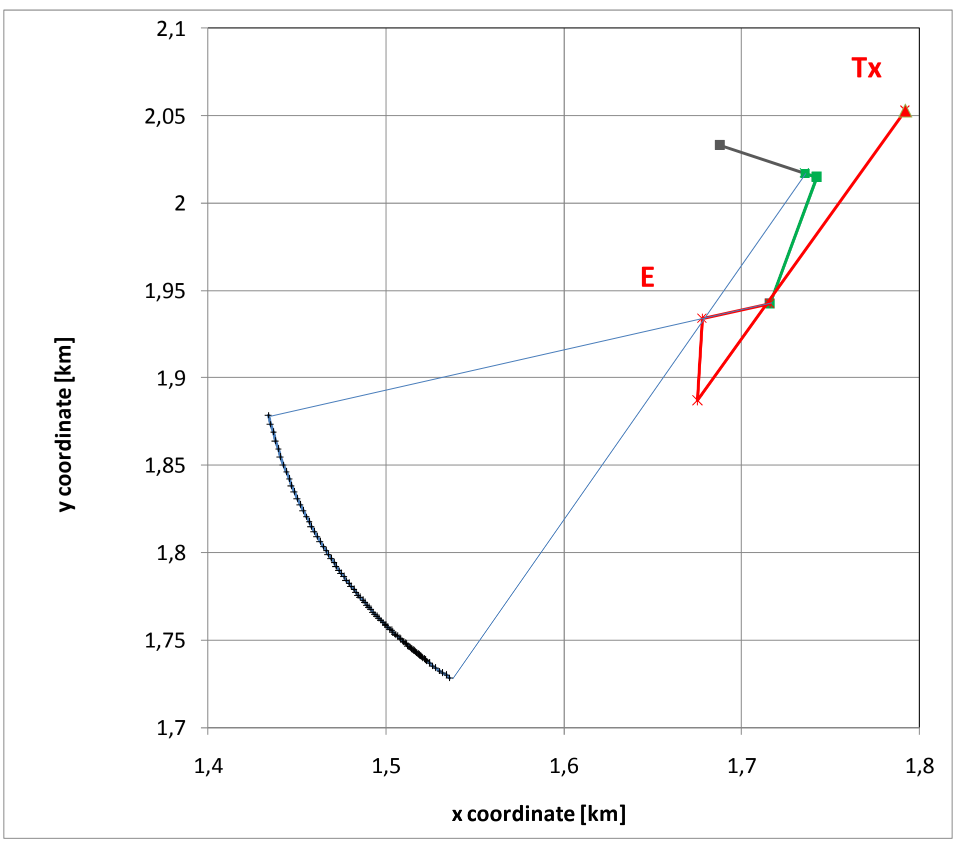

Fig. 9. Ground plan of Fig. 4. (L-shaped route 2) containing only features relevant for sample entity with visibility of 86 m. Red triangle - Tx; red line - ray path with two interactions; grey line (partially covered with green one) - 135 m long Rx route; green line - "entity visible" section; blue line - locus of virtual Tx along the entity. Note that thin blue lines connect end points of visible section with appropriate virtual Tx. Markers on blue line denote virtual Tx-es for Rx locations sampled at 1m along the Rx route. Note that last interaction point (point E) is stationary for the entity only on the ground plan, but not in its height.

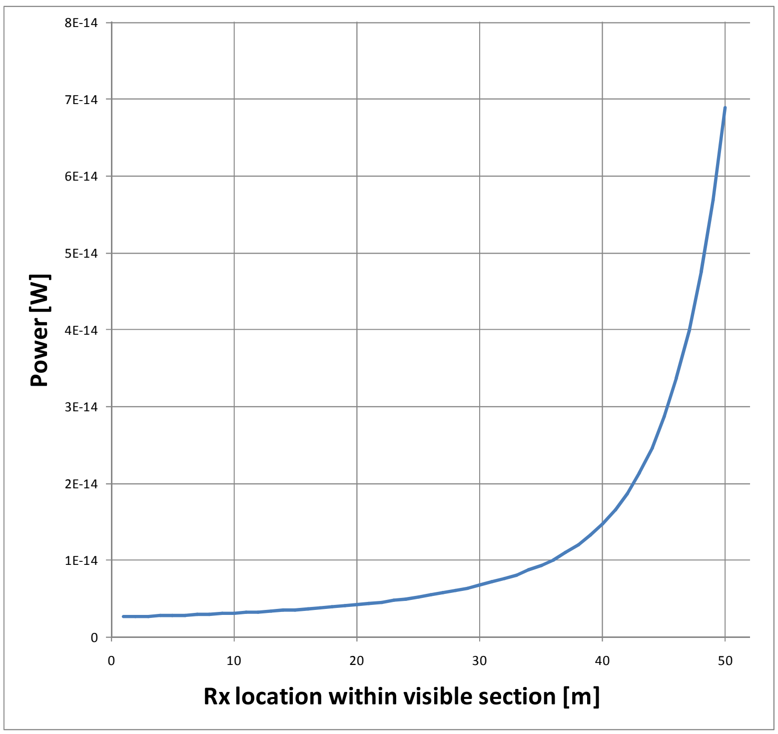

(a)

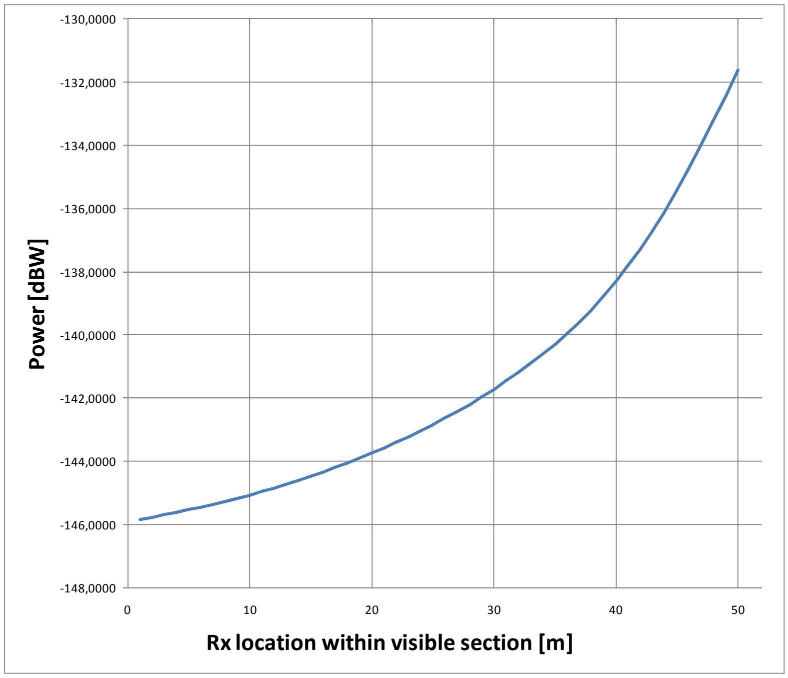

(b)

Fig. 10. Power curve in W (a) and dBW (b) along the 50m long entity visibility section. Such curves can be easily approximated with polynomials.

Fig. 10. gives the ray power at Rx location along the route section where the entity is visible which can be represented with few-element polynomials. Fig. 11. gives the interpolated ray power along the 50m long entity. Interpolation i.e. curve fitting was done with 4^{th} (a) and 5^{th} (b) degree polynomial fit. This way for a negligible residual fit error instead of storing 50 data points only 4 or 5 polynomial coefficients are stored.

Table 2 gives all values needed and stored for each ray entity for future reconstruction, i.e. interpolation of rays. Procedure of finding rays present at a given arbitrary receiver location using ray entity data is rather simple. Firstly, algorithm finds all entities present at that location. Then from parameters that describe ray entity and from locations of Tx and Rx all rays properties can be recalculated. For example, through x and y coordinates of last interaction, entity delay offset, location of Rx and Tx virtual Tx location can be determined using simple geometry, and then angles of departure and arrival and time delay follow. Power is interpolated by finding relative location of desired Tx within the entity (using entity data about its start point) and polynomial interpolation.

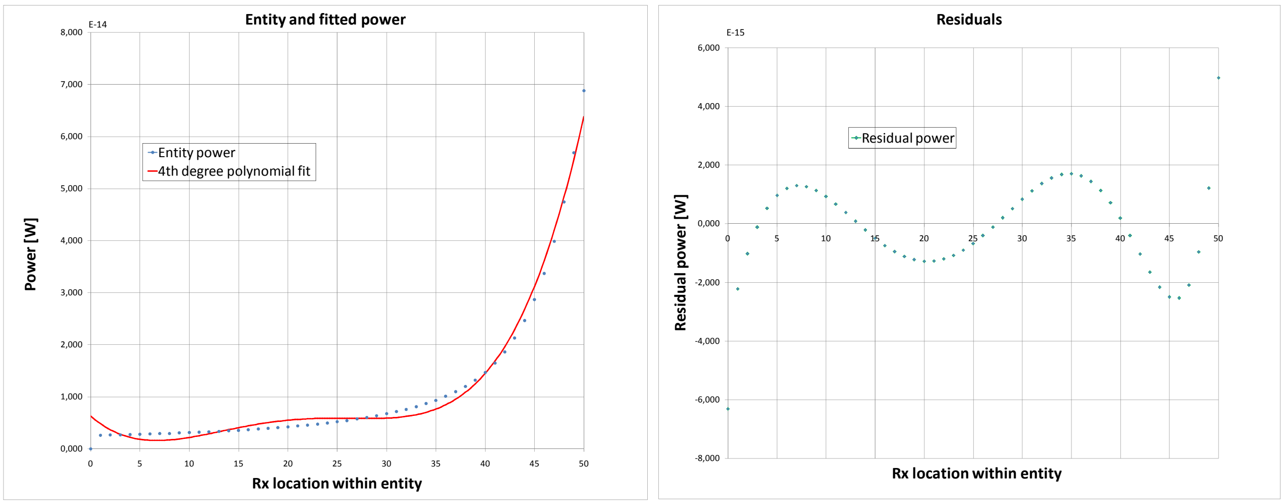

(a)

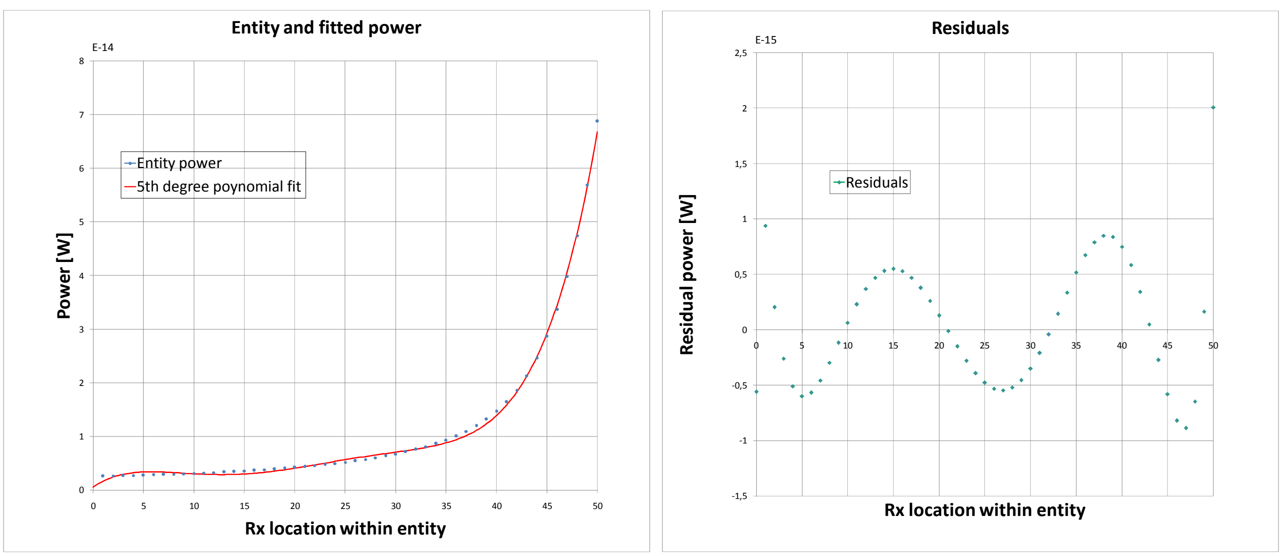

(b)

Fig. 11. Interpolated received power for a specific entity 50m long. Curve fitting is depicted for 4^{th} degree polynomial (a) and 5^{th} degree polynomial (b)

The 4th degree polynomial has SSE (Sum of Squared Errors) 9.81E-29 with R-square (coefficient of determination) 0.9906 and RMSE (Root Mean Square Error) 1.477E-15. 5th degree polynomial has SSE 1.557E-29 with R-square 0.9985 and RMSE 5.95-16. It should be noted however that the average received power for 50 samples is 1.155E-14 W.

If we exclude the first sample due to Runge's phenomenon then for the 4th degree polynomial fit maximum residual value (difference between polynomial fit and actual value) is 2.576 dB, the minimum residual value is 0.053 dB with average residual value of 0.766 dB. For the 5th degree polynomial fit maximum residual value 0.845 dB, the minimum residual value is 0.0023 dB with average residual value of 0.307 dB. From the given results it can be seen that it's advisable to use the 5th degree polynomial fit for received power interpolation.

Table 2. Comparison of numbers of entities and number of rays, and corresponding number of values needed to describe them

	Number of rays	Number of entities
no power threshold example	26176	1221
power threshold example	16456	844
Values necessary to describe a ray/entity	Ray • Ray length/time delay • elevation angle • azimuth angle • Ray arrival location (integer index) • Ray power	Entity • entity start (integer index) • entity end (integer index) • entity delay offset (i.e. virtual Tx locus radius) • last interaction (edge) x-y coordinates (point E in fig. 8),

		to ensure calculation of correct virtual Tx on a circle, for each Rx • Entity power polynomial interpolation (5 coefficients)
Values total	For Ray: 4 real + 1 integer	For Entity: 8 real + 2 integer

Table 3. Comparison between classical ray-tracing and ray entity based interpolation methods

	Simple Ray Tracing	Entity Interpolation RT
Memory usage	Higher (11-12 times)	Lower (11-12 times)
Rx Resolution (number of receivers at a certain area)	Fixed after initial RT run	Unlimited (can be increased arbitrarily after initial RT run)
Computational burden for increased Rx resolution	Increasing significantly	Negligible increase
Versatility for including other effects (over the rooftop diffraction, diffuse scattering)	YES	YES, with simple adaptation for each effect

Representation of ray tracing simulations by ray entities can reduce memory usage, and interpolation by virtue of rays sorted in ray entities enables more refined results at small additional computational cost. Reduced memory requirement can be argued by Table 2., which gives comparison in two examples of L-shaped route scenario with and without power threshold imposed on rays. It shows that storing ray tracing simulation as ray entities would require less than a double memory per entity as per ray. Significant memory reduction is expected since number of entities is significantly smaller then number of rays; in two examples given, the reduction is 19.5-21.4 times. Thus the overall memory usage reduction is about 11-12 times. The table 2. gives values only for diffraction cases from two reasons. Firstly, because three simulations considered, as the most of typical urban environments, were dominated by diffraction. Secondly, REs based on pure reflections have a stationary virtual Tx, thus making their recording even simpler and less memory consuming. Only a dubious and hard to imagine case of environment dominant by many ray entities of very short duration along the receiver path could see no improvement or even disadvantage in memory usage when using RE approach.

Table 3. sums up all features of comparison between classical ray-tracing and ray entity based interpolation method. Although reduced memory usage for a factor of 11 may look as an interesting feature, the major advantage of this approach is the ability to interpolate RT results to arbitrary high resolution. This feature is available after initial RT simulation and after post-processing is performed. This method can be repeated for customized needs of the user. Thus, ray entity introduction enables simulations of radio channel with arbitrarily moving user, with arbitrary modulation and coding scheme, in wide frequency band range and with sufficient spatial resolution. This can be used for deterministic reference channel model of computer efficiency comparable to its stochastic based counterparts, but with much more realistic and standardized performance.

5. Conclusion

The paper introduced a novel concept of ray entities as a versatile interpretation and post-processing of ray tracing data simulated in urban, rich multipath environments. It is hypothesized that combining of rays that undergo same propagation phenomenon into one entity can be of some benefit for reduced storage of ray data and may enable interpolation of ray tracing results.

Examples given in the paper have shown that memory needed to store ray tracing results was reduced by a factor of around 11 to 12. Further investigation with more case studies is needed for more accurate value of reduced memory requirements, but it is clear that there will always be some reduction except in cases of large number of short entities, which is physically unfeasible except maybe in rare architectural cases. Since examples in the paper were dominated by diffraction, even more reduction can be expected in reflection rich environments, where ray entity's virtual source is stationary.

The existence of ray entities and insight into their nature, such as dynamics of their power, angle of arrival and their visibility area can improve understanding of urban multipath environments and inspire adapting radio system aspects to that understanding. For example, some adaptive beam forming or MIMO system could be designed having in mind facts about continuous change of arriving rays properties, as mobile user is moving along an entity.

Ray entity concept also enables interpolation of ray tracing results obtained for sufficiently closely located set of receivers. It enables, at negligible computational cost, obtaining of ray tracing data of arbitrary high resolution.

Finally, ray entity concept is a step towards feasible deterministic reference channel model, a standardized channel model that would have database of RT-simulated typical environments, recorded in ray entity format. Next step would be to use similar algorithm and detect ray entities as 2D surfaces, interpolate powers in 2D and to simulate a complete urban area with some arbitrary Tx resolution. This would enable users, who want to test and compare various wireless system concepts on a real environment, to do so in more realistic way than it is the case with currently available stochastic-based reference channel models.

ACKNOWLEDGMENT

The 3D ray tracing tool used in this paper was developed at University of Bologna in a group of prof. Vittorio Degli Esposti. The authors thank him for his kind cooperation.

REFERENCES

P. Almers et al., (2007), Survey of Channel and Radio Propagation Models for Wireless MIMO Systems, EURASIP Journal on Wireless Communications and Networking, vol. 2007, article ID 19070, 19p.

H. Asplund et al., (2006), The COST 259 Directional Channel Model – Part II – Macrocells, IEEE Transactions on Wireless Communications, Vol. 5, No. 12, pp. 3434-3450.

L. M. Correia (Ed.), (2006), Mobile Broadband Multimedia Networks (Techniques, Models and Tools for 4 G), Elsevier, Amsterdam.

V. Degli-Esposti, D. Guiducci, A. de'Marsi, P. Azzi, F. Fuschini, (2004), An advanced field prediction model including diffuse scattering, IEEE Transactions on Antennas and Propagation, Volume 52, Issue 7, pp:1717 – 1728.

F. Fuschini, H. El-Sallabi, V. Degli-Esposti, L. Vuokko, D. Guiducci, P. Vainikainen, (2008), Analysis of multipath propagation in urban environment through multidimensional measurements and advanced ray tracing simulation, IEEE Transactions on Antennas and Propagation, Vol. 56, No. 3, Page(s):848 – 857.

K. Haneda, J. Poutanen, F. Tuvfesson, L. Liu, V. Kolmonen, P. Vainikainen, and C. Oesteges, (2011), Development of multi-link geometry-based stochastic channel models, Proc. Antennas and Propagation Conference (LAPC), pp.1-7.

A. Katalinić Mucalo, R. Zentner, and N. Mataga, (2012), Benefits and Challenges of Deterministic Reference Channel Models", Automatika, vol. 53, no. 1, pp. 80-87.

A. Katalinić Mucalo, R. Zentner, (2011), Microscopic Level of Visibility Regions for Urban Environment Scenarios, *Proc. 5th European Conference on Antennas and Propagation*, pp. 2042-2046.

J.B. Keller, Geometrical Theory of Diffraction, (1962), J. Opt. Soc. of America, Vol.52, No.2, pp. 116-130.

D.A. McNamara, C.W.I. Pistorius, J.A.G. Malherbe, (1990), Introduction to the Uniform Geometrical Theory of Diffraction, Artech House, Boston London.

Molisch et al., (2006), The COST 259 Directional Channel Model – Part I – Overview and Methodology, IEEE Transactions on Wireless Communications, Vol. 5, No. 12, pp. 3421-3433.

I. Sirkova, (2006), Overview of COST 273 Part I: propagation modelling and channel characterization, Proc. of the XLI International Conference on Information, Communication and Energy Systems and Technologies (ICEST), pp. 29-32, Sofia (Bulgaria), 29th June.

R. Zentner, A. Katalinić Mucalo, T. Delač, (2013), Virtual Source Modeling for Diffraction in Reference Channel Modeling, Proc. 7th European Conference on Antennas and Propagation.

FIGURES

TABLES

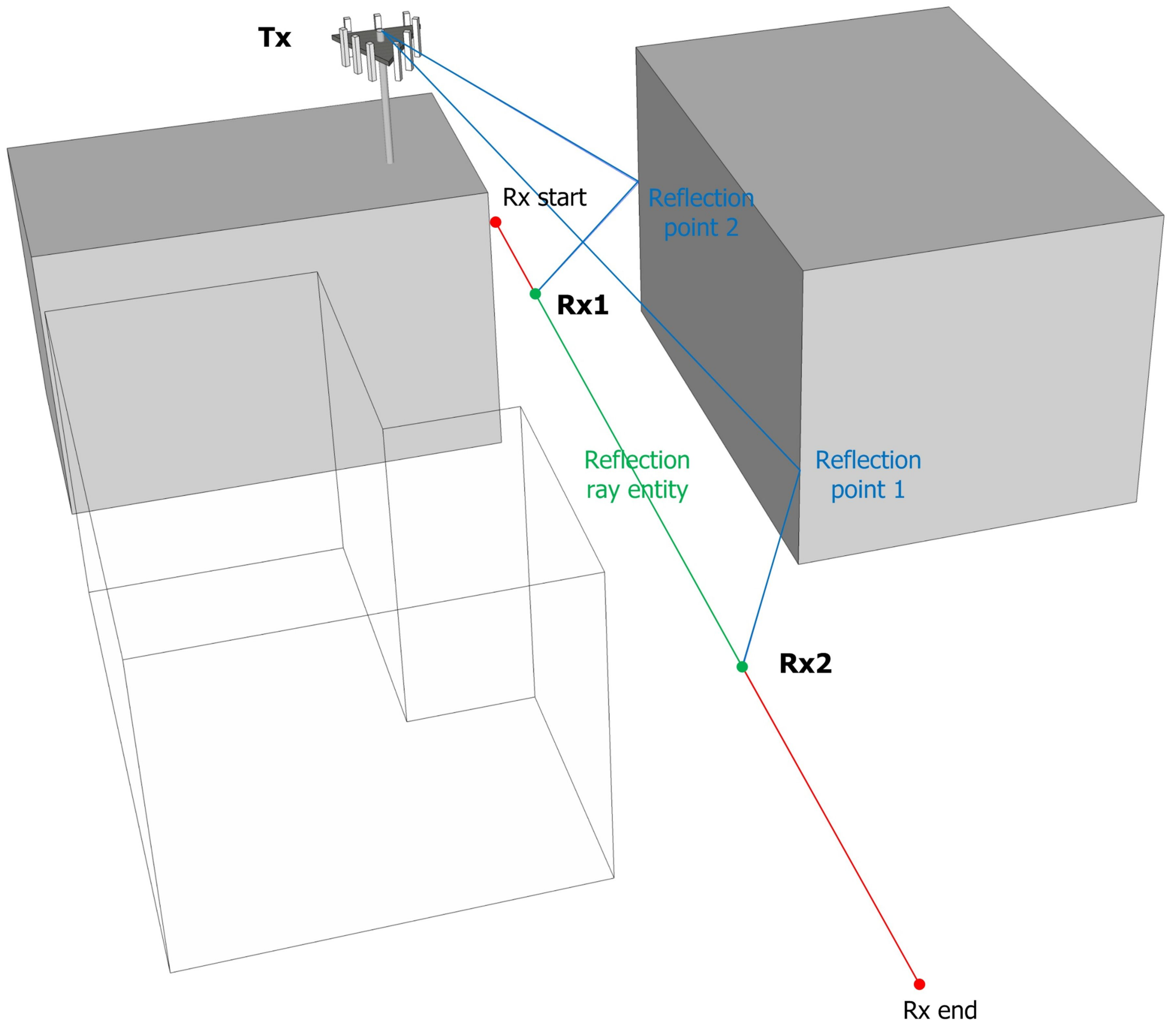
Tx
Rx start
Reflection
point 2
Rx1
Reflection
ray entity
Reflection
point 1
Rx2
Rx end

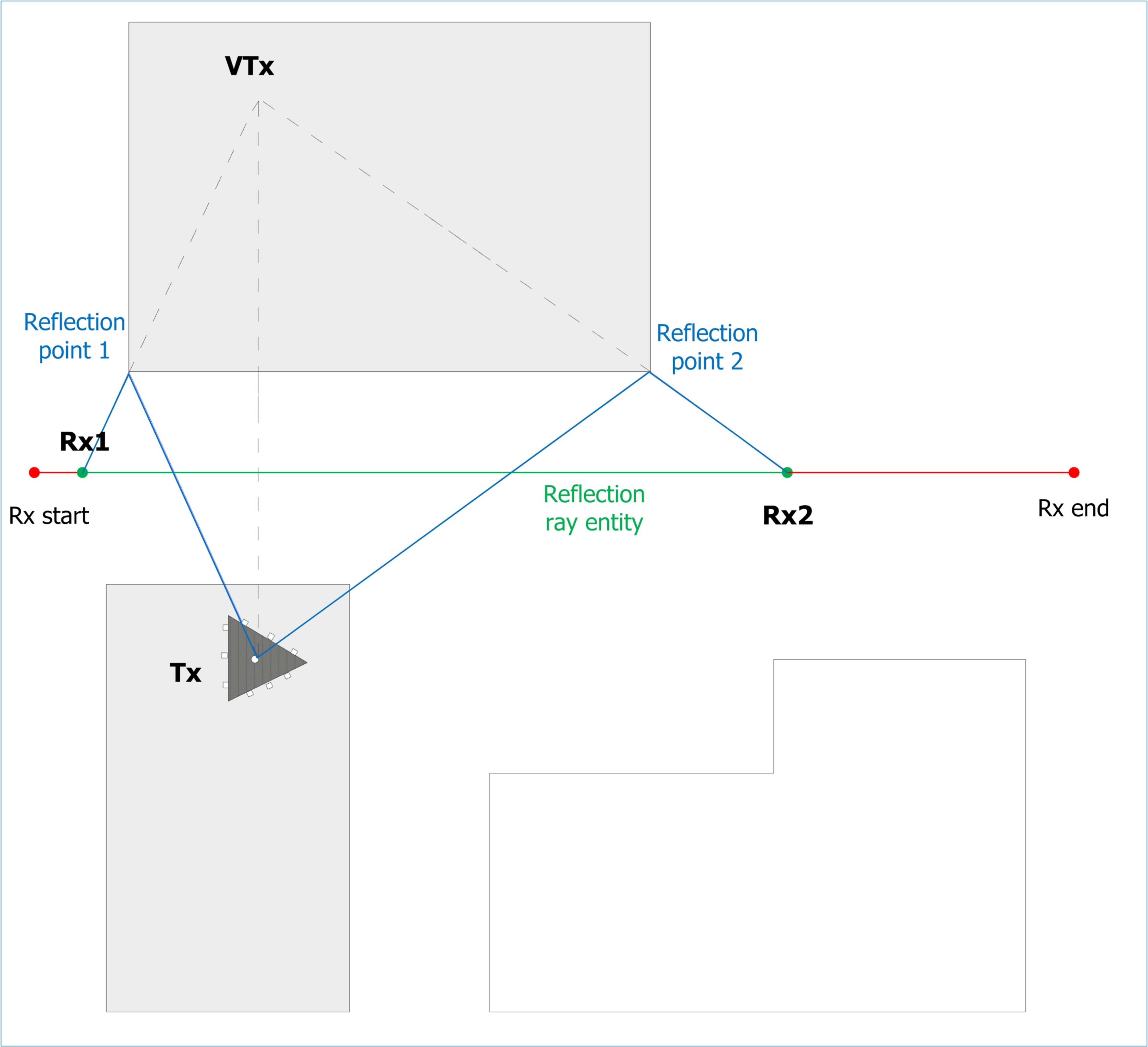
VTx
Reflection point 1
Reflection point 2
Rx1
Rx start
Reflection ray entity
Rx2
Rx end
Tx


Tx
Diffraction point 1
Diffraction point 2
Rx start
Rx3
Edge A
Edge C
Edge B
Diffraction ray entity
Rx4
Rx end

Rx3
Diffraction
ray entity
Rx4
Rx start
Rx end
Edge C
Edge B
Tx
Edge A
Diffraction
point 1, 2
Vtx2
Vtx1

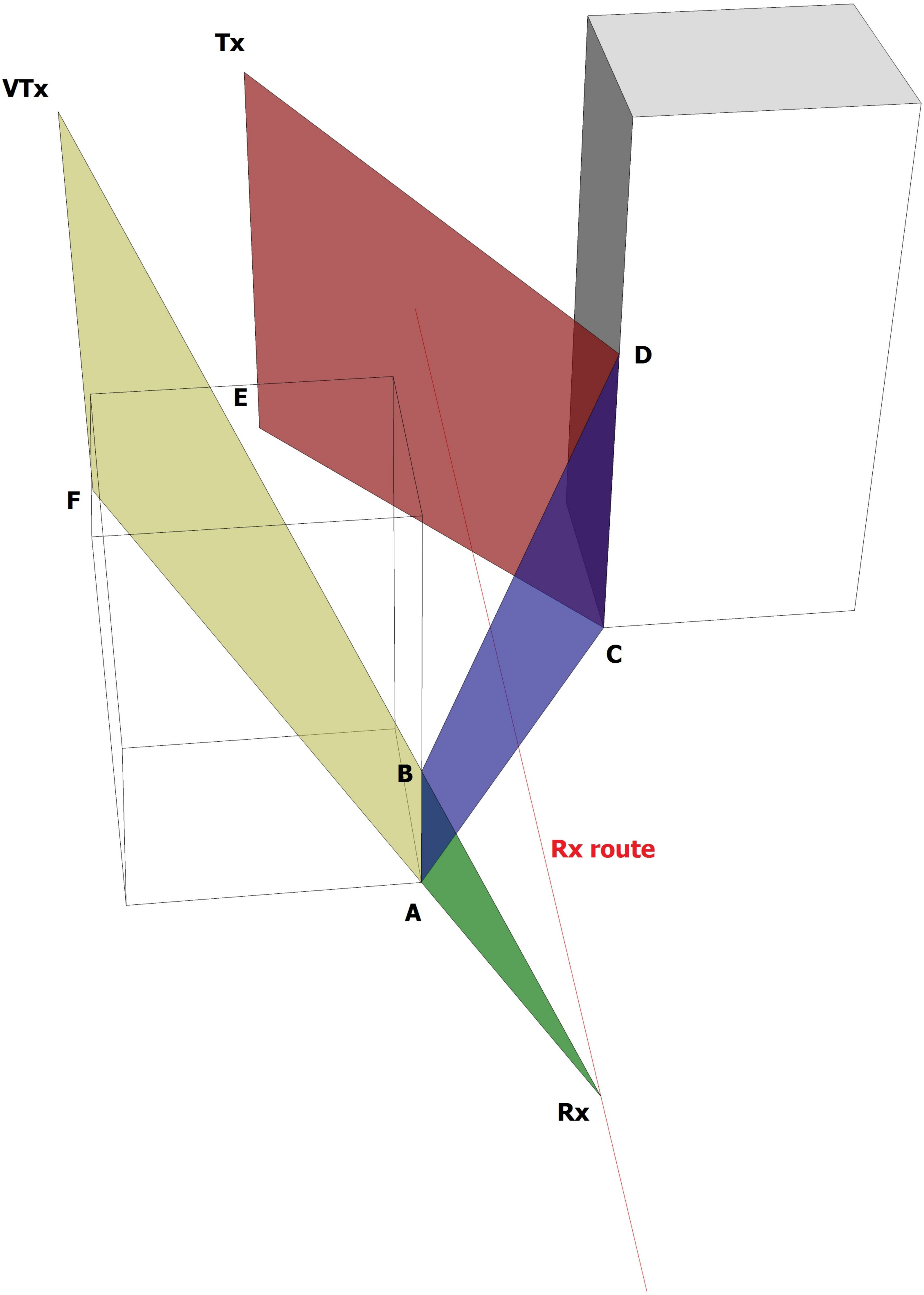
Tx
VTx
D
E
F
C
B
Rx route
A
Rx

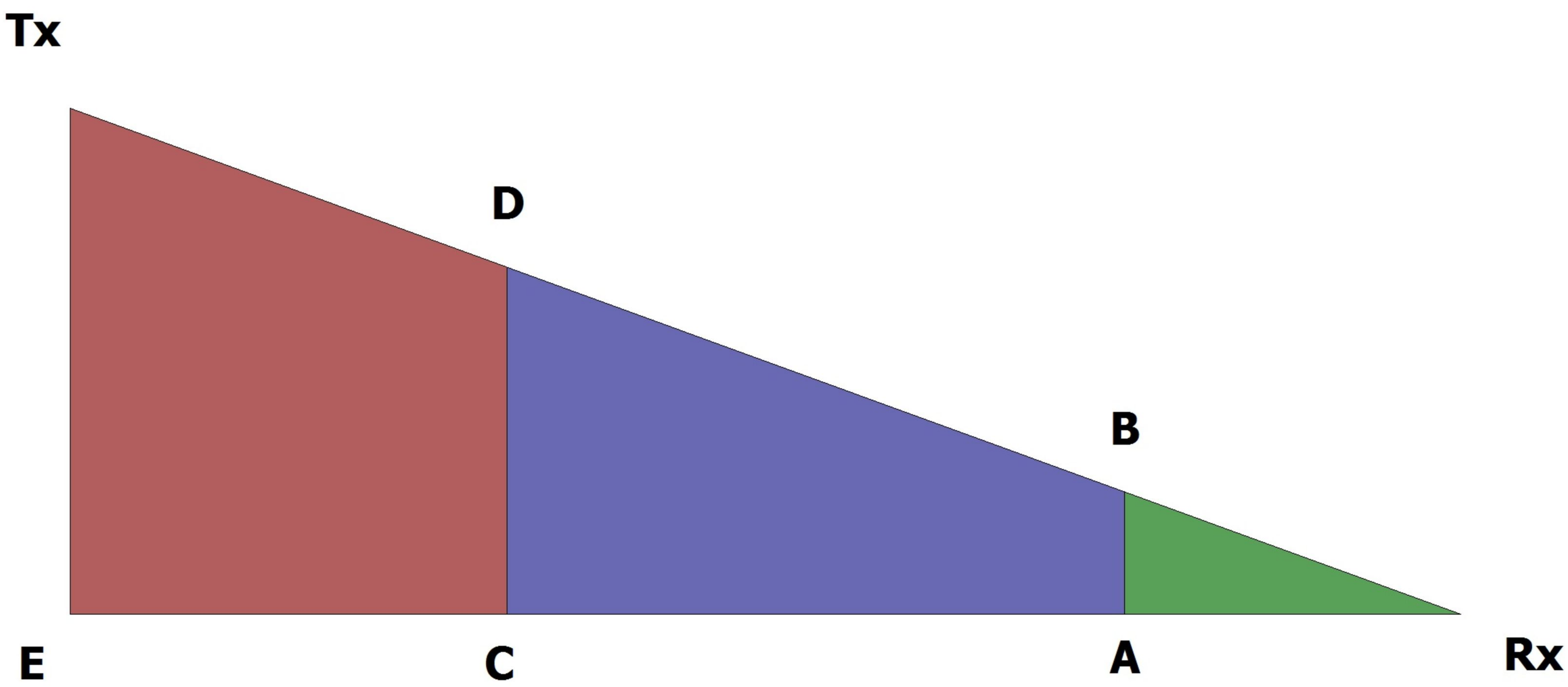
Tx
D
B
E
C
A
Rx

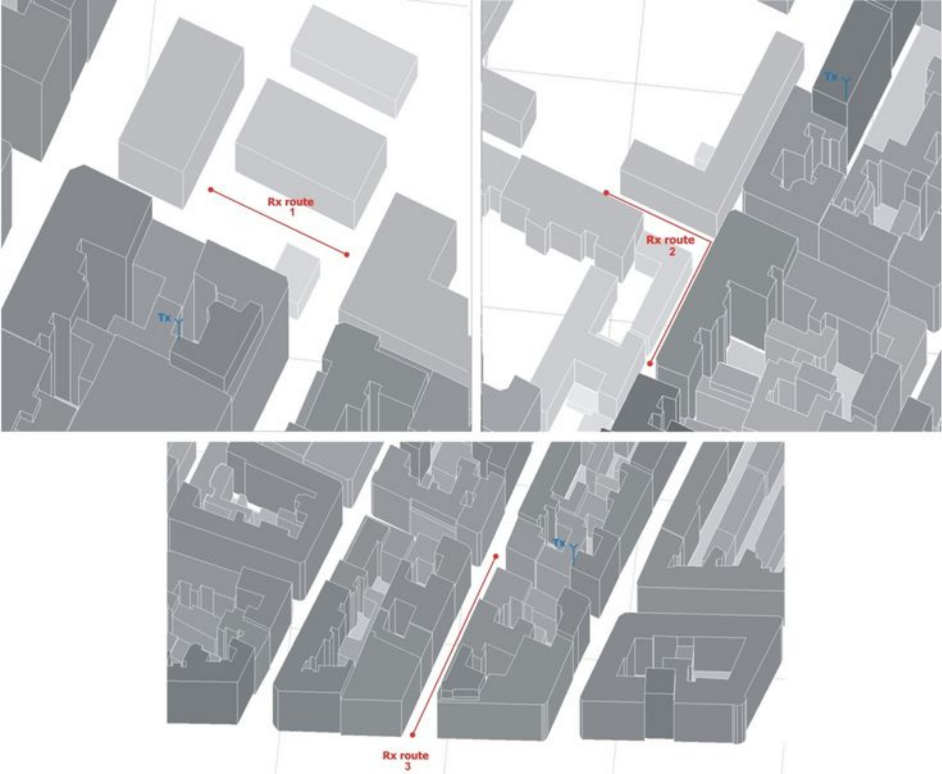
Rx route 1
Tx
Tx
Rx route 2
Tx
Rx route 3

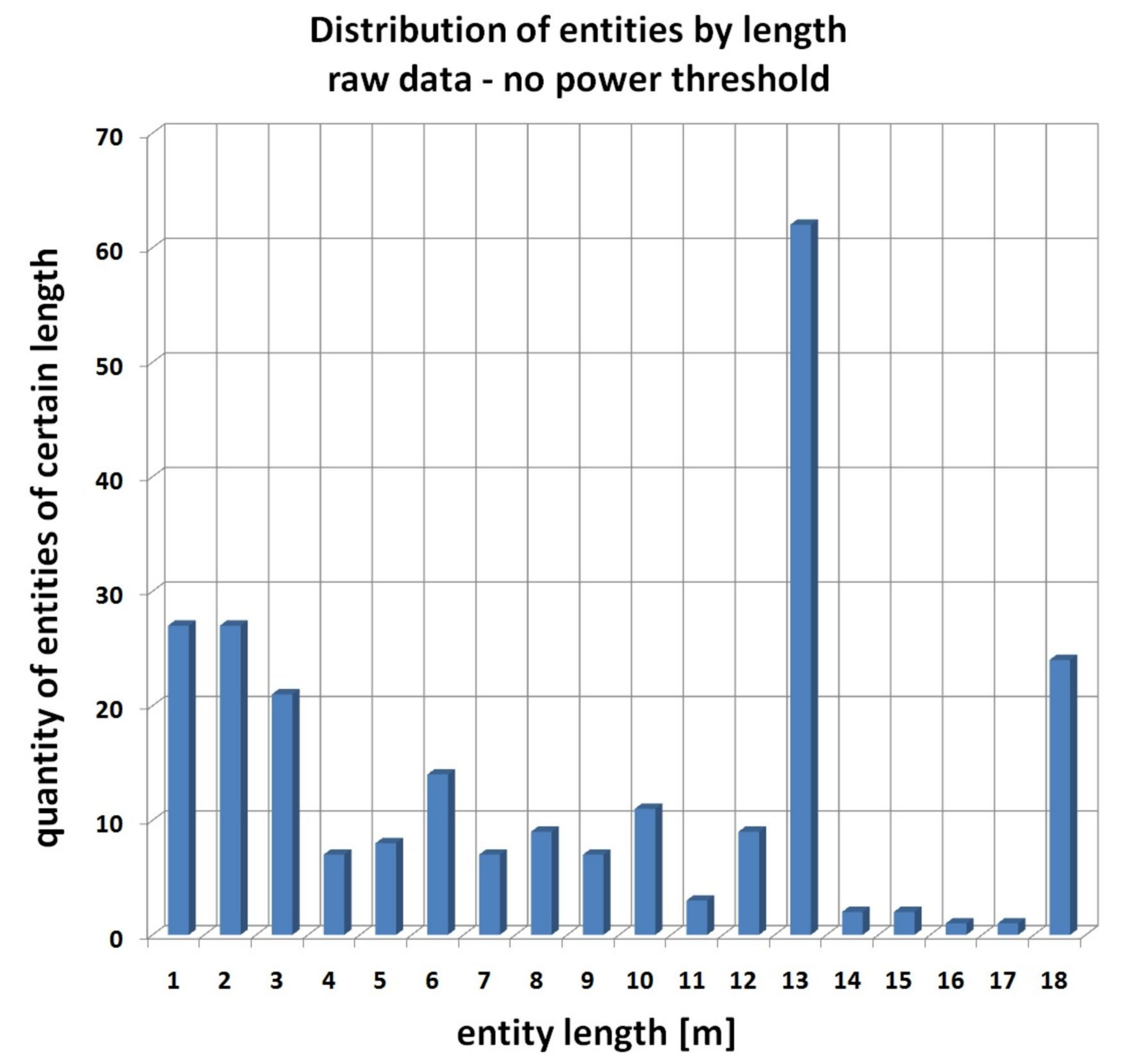
Distribution of entities by length
raw data - no power threshold
quantity of entities of certain length
0
10
20
30
40
50
60
70
1
2
3
4
5
6
7
8
9
10
11
12
13
14
15
16
17
18
entity length [m]

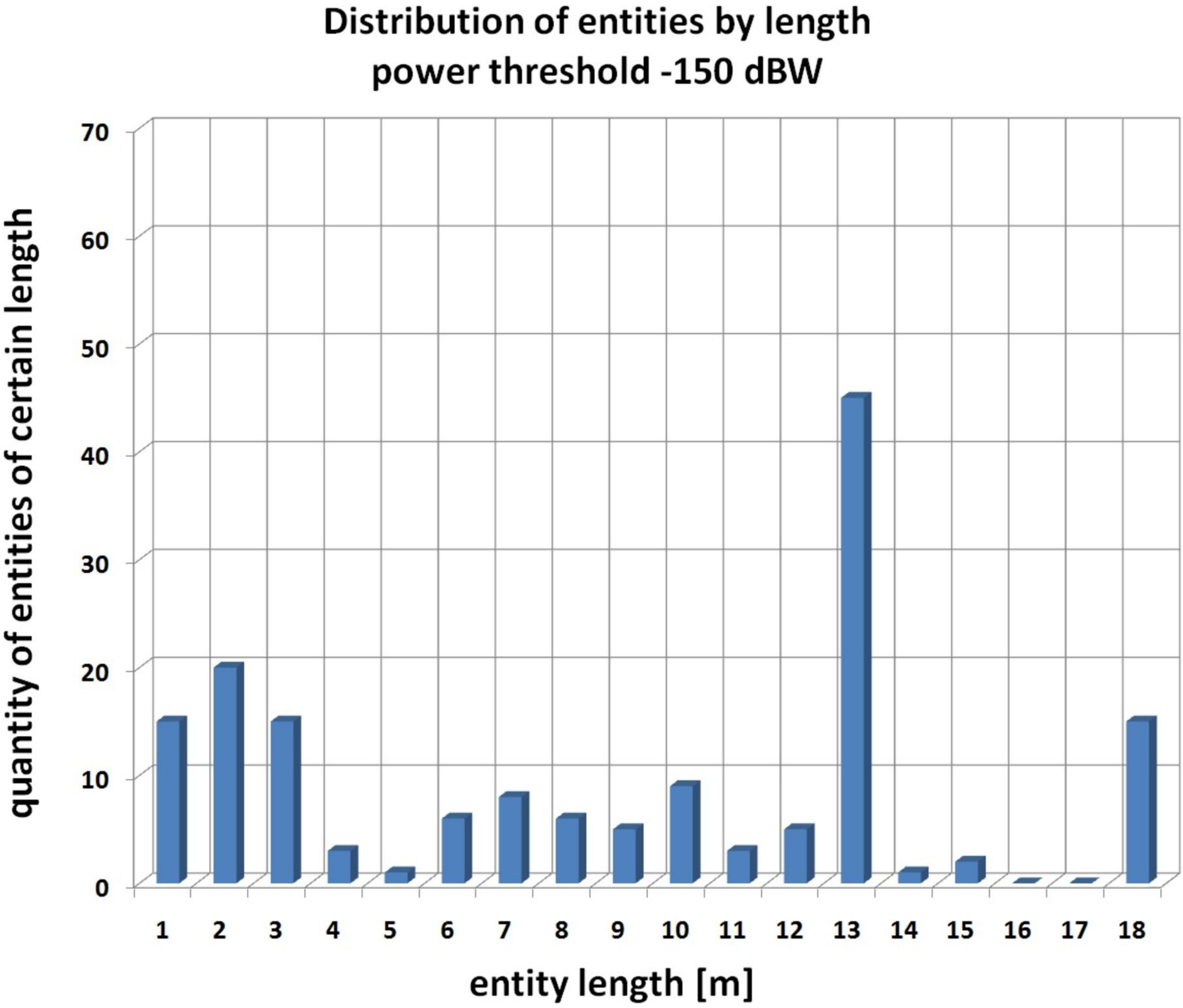
Distribution of entities by length
power threshold -150 dBW
quantity of entities of certain length
0
10
20
30
40
50
60
70
1
2
3
4
5
6
7
8
9
10
11
12
13
14
15
16
17
18
entity length [m]

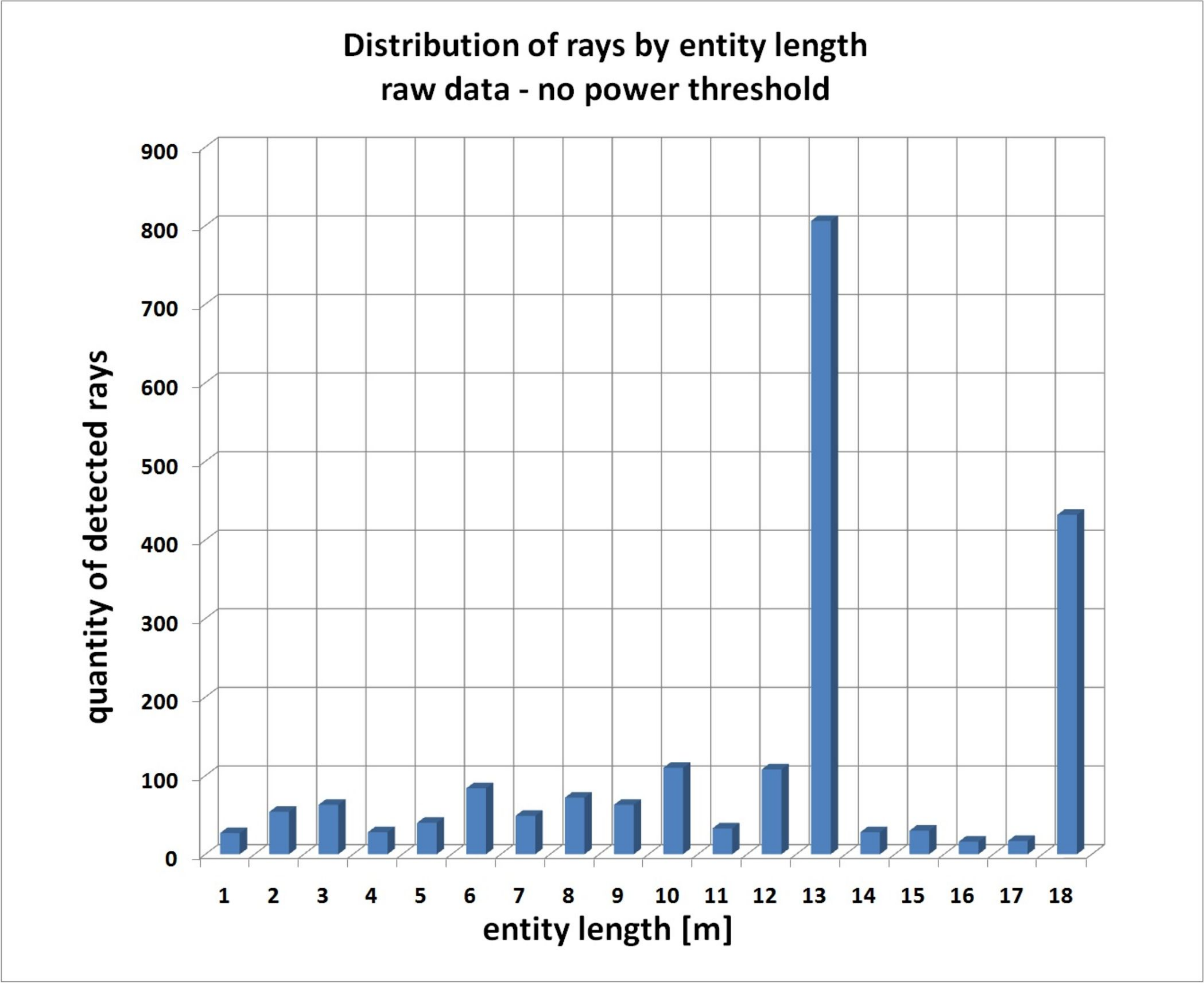
Distribution of rays by entity length
raw data - no power threshold
quantity of detected rays
0
100
200
300
400
500
600
700
800
900
1
2
3
4
5
6
7
8
9
10
11
12
13
14
15
16
17
18
entity length [m]

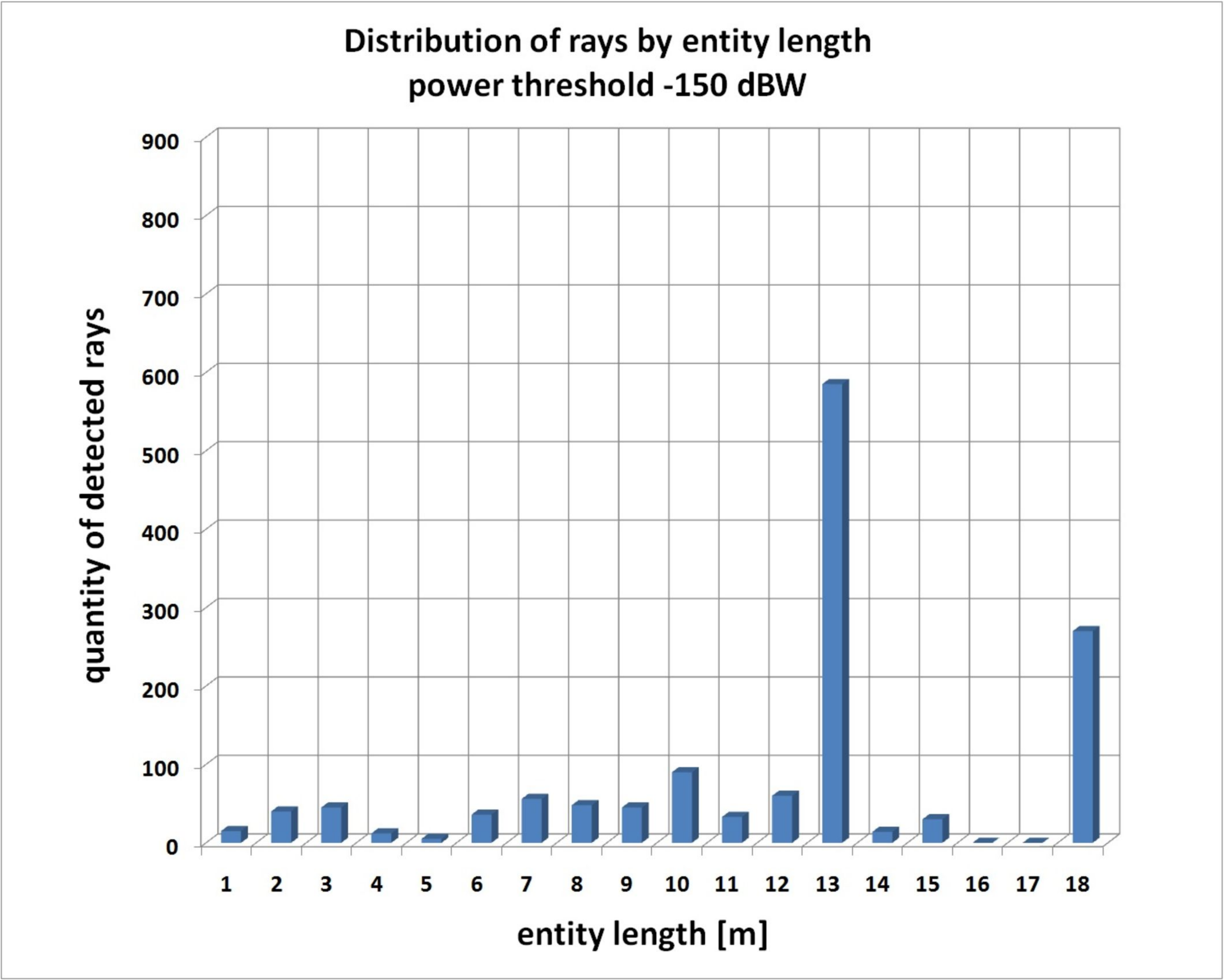
Distribution of rays by entity length
power threshold -150 dBW
quantity of detected rays
900
800
700
600
500
400
300
200
100
0
1
2
3
4
5
6
7
8
9
10
11
12
13
14
15
16
17
18
entity length [m]

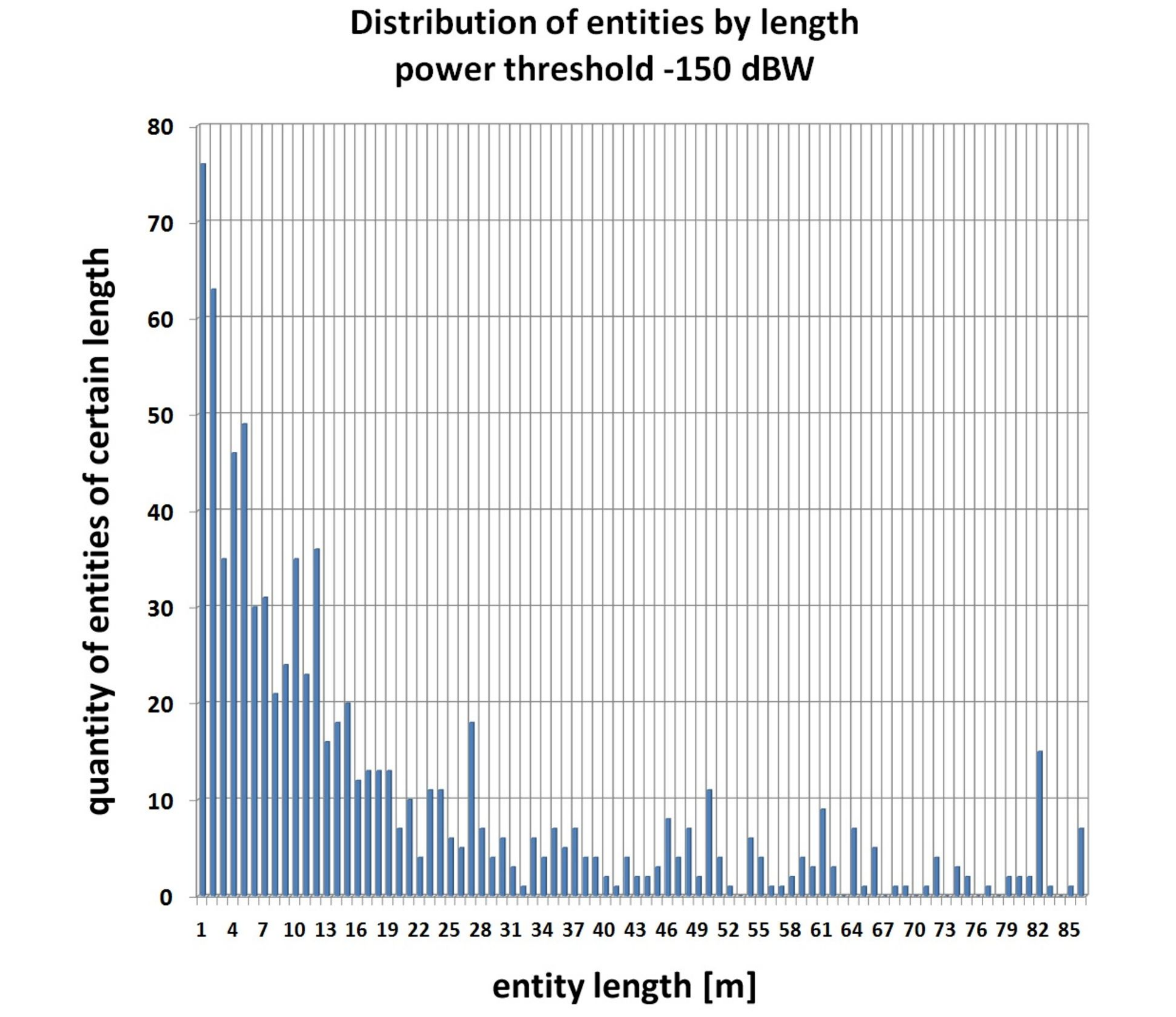

Distribution of entities by length
power threshold -150 dBW
quantity of entities of certain length
entity length [m]
0
10
20
30
40
50
60
70
80
1 4 7 10 13 16 19 22 25 28 31 34 37 40 43 46 49 52 55 58 61 64 67 70 73 76 79 82 85

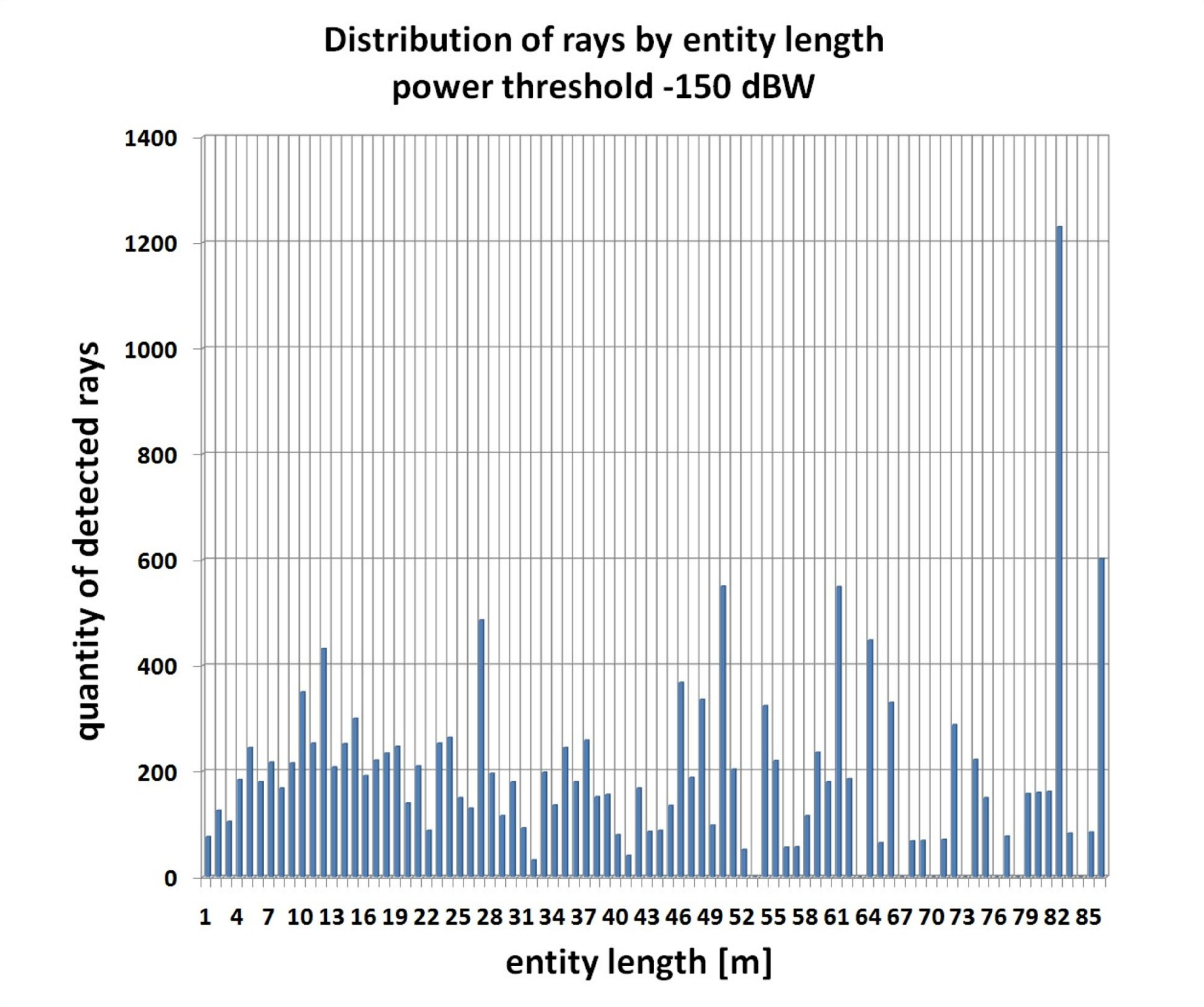
Distribution of rays by entity length
power threshold -150 dBW
quantity of detected rays
entity length [m]
0
200
400
600
800
1000
1200
1400
1 4 7 10 13 16 19 22 25 28 31 34 37 40 43 46 49 52 55 58 61 64 67 70 73 76 79 82 85

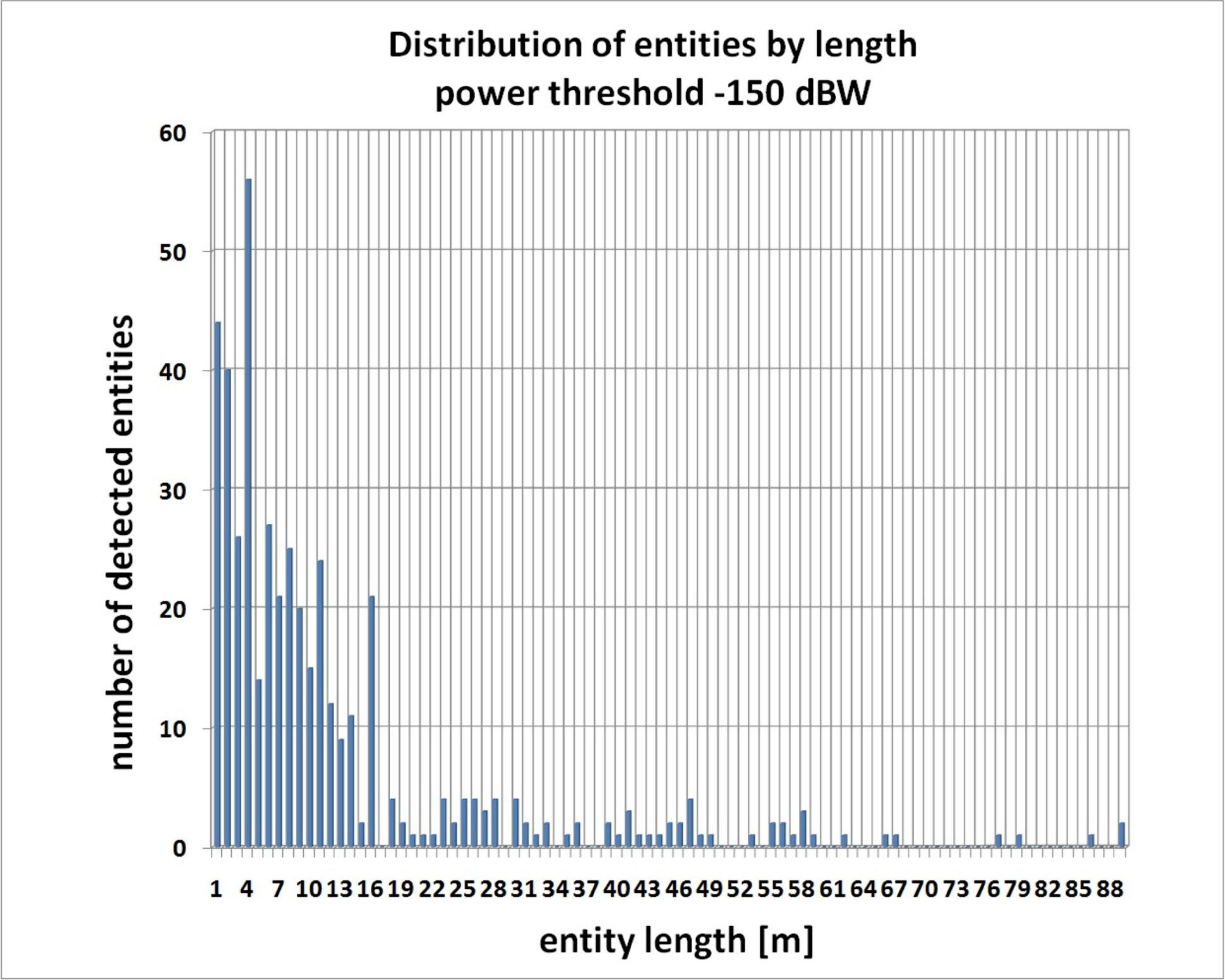

Distribution of entities by length
power threshold -150 dBW
number of detected entities
entity length [m]
0
10
20
30
40
50
60
1 4 7 10 13 16 19 22 25 28 31 34 37 40 43 46 49 52 55 58 61 64 67 70 73 76 79 82 85 88

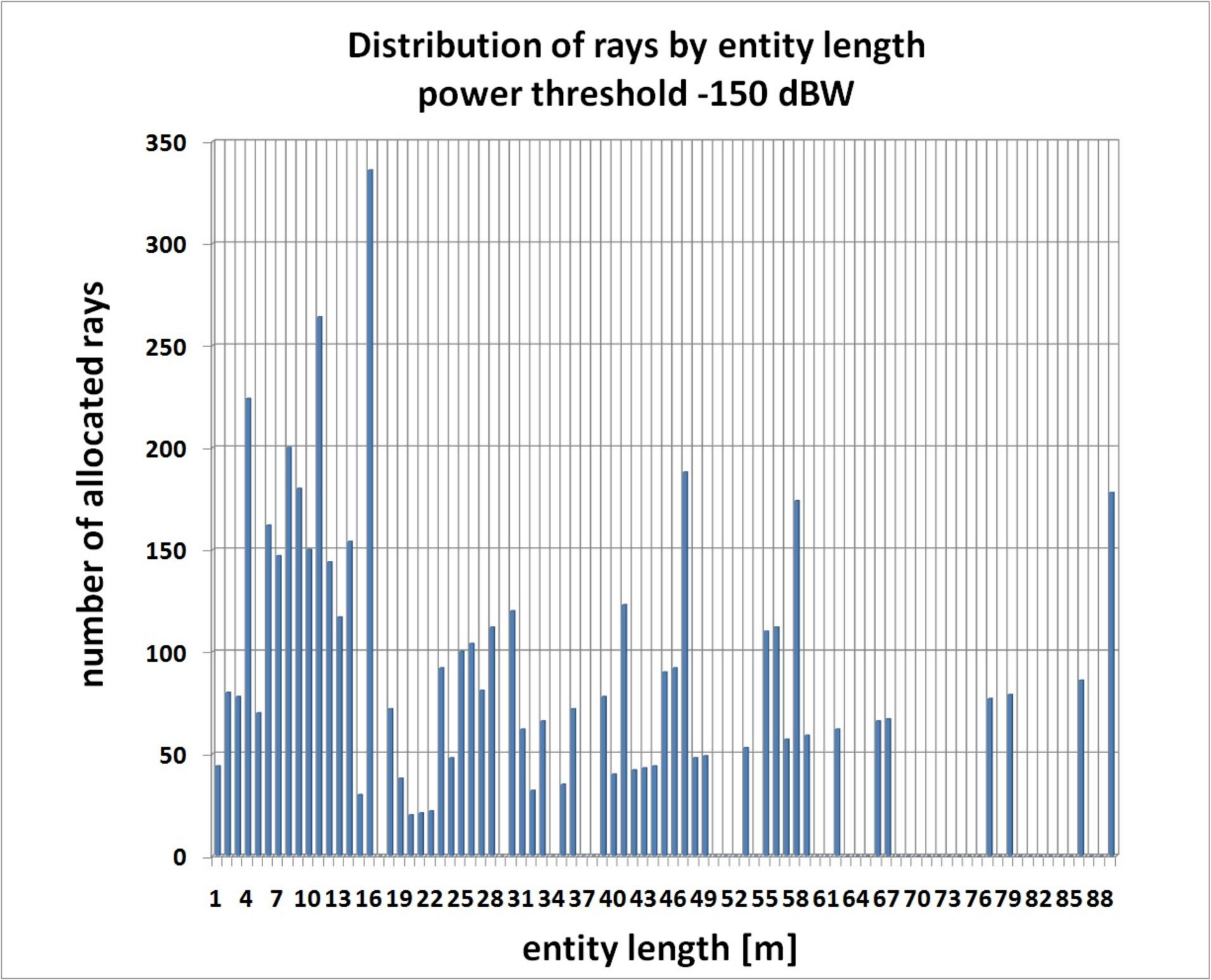

Distribution of rays by entity length
power threshold -150 dBW
350
300
250
200
150
100
50
0
number of allocated rays
1 4 7 10 13 16 19 22 25 28 31 34 37 40 43 46 49 52 55 58 61 64 67 70 73 76 79 82 85 88
entity length [m]

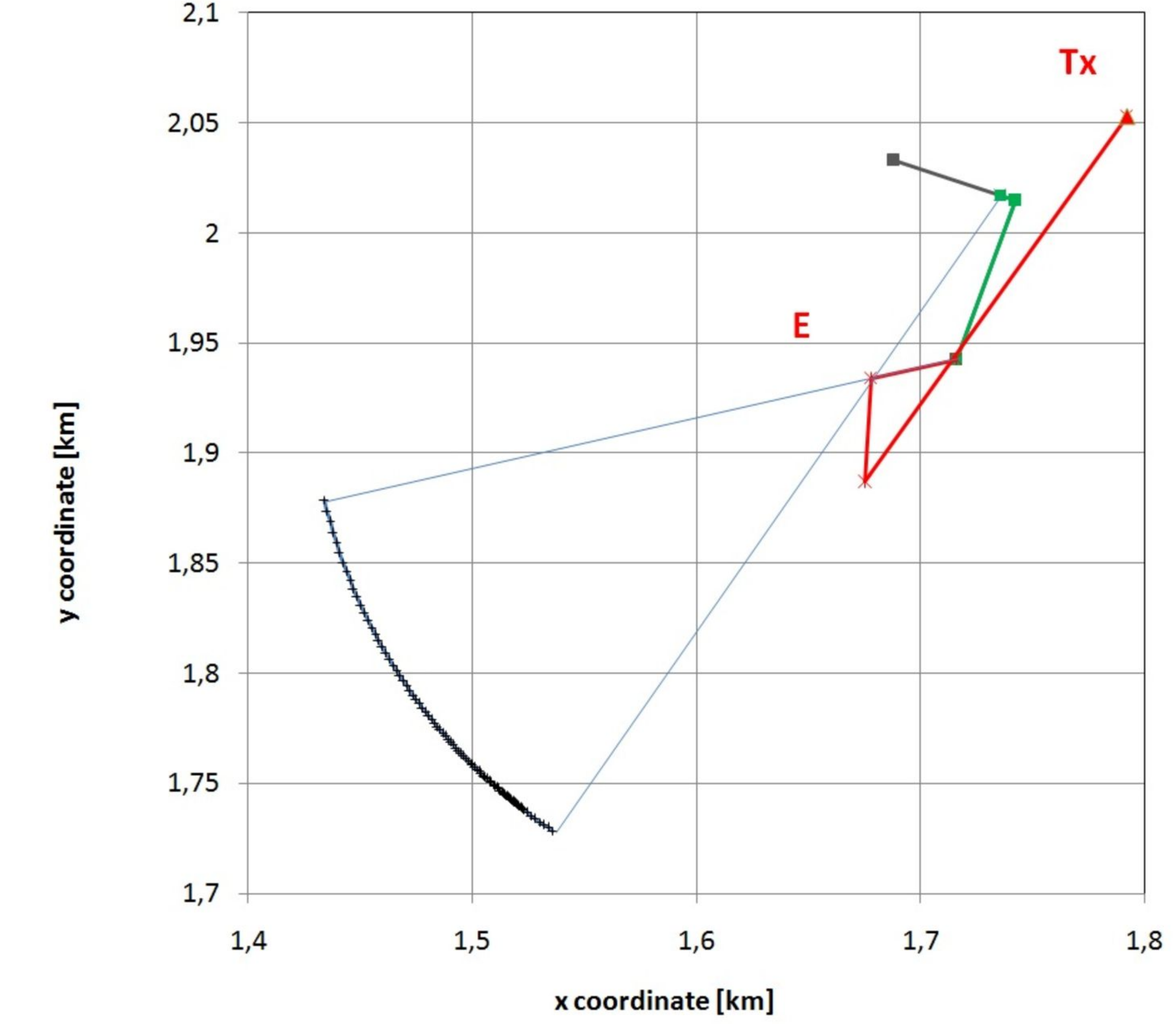

Tx
E
2,1
2,05
2
1,95
1,9
1,85
1,8
1,75
1,7
1,4
1,5
1,6
1,7
1,8
y coordinate [km]
x coordinate [km]

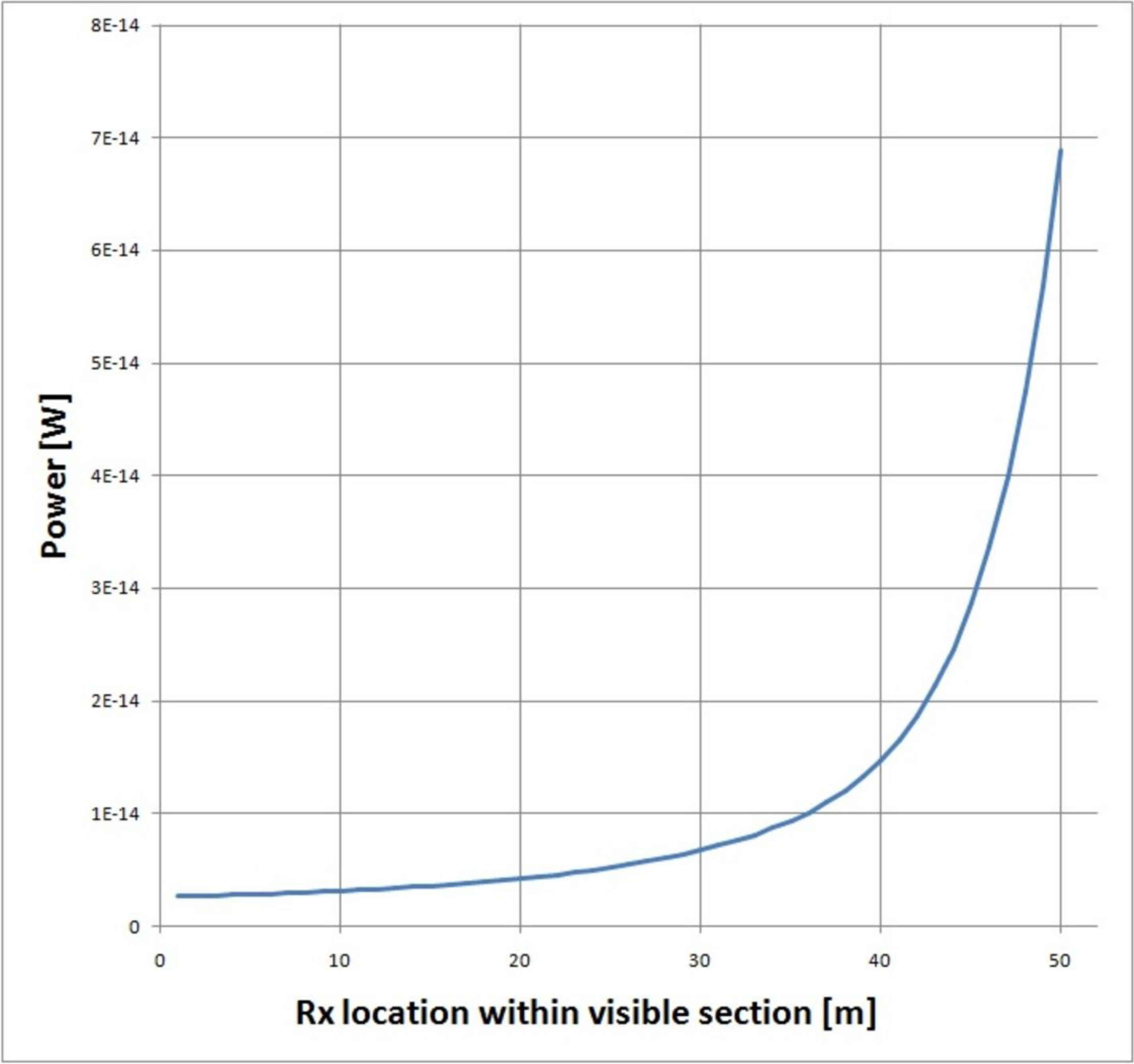

Power [W]
8E-14
7E-14
6E-14
5E-14
4E-14
3E-14
2E-14
1E-14
0
0
10
20
30
40
50
Rx location within visible section [m]

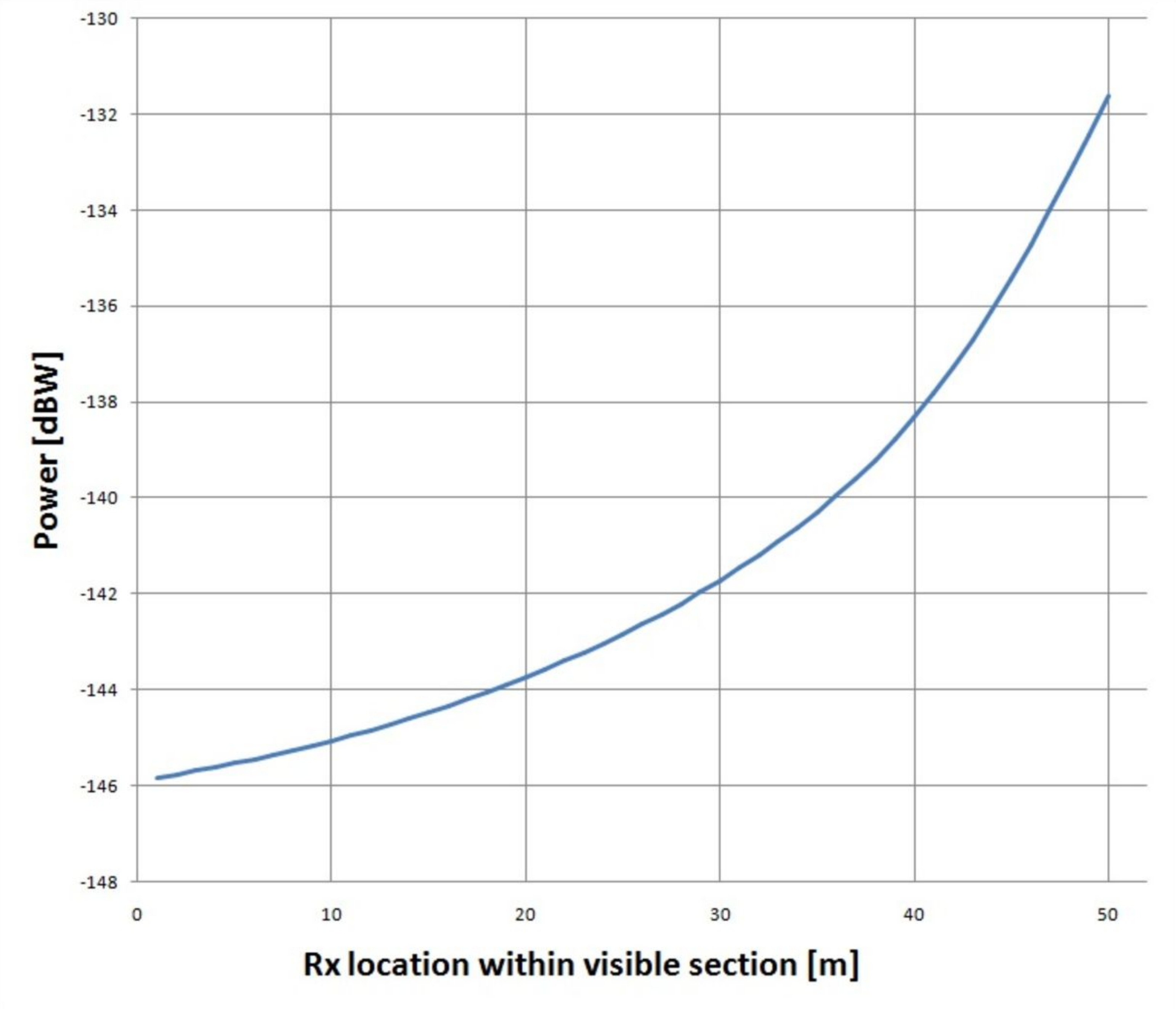
Power [dBW]
-130
-132
-134
-136
-138
-140
-142
-144
-146
-148
0
10
20
30
40
50
Rx location within visible section [m]

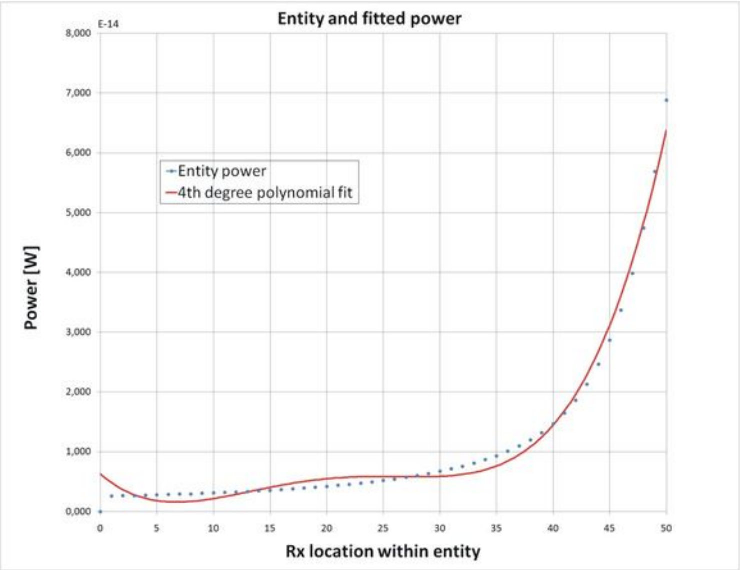
Entity and fitted power
E-14
8,000
7,000
6,000
5,000
4,000
3,000
2,000
1,000
0,000
Power [W]
Entity power
4th degree polynomial fit
0
5
10
15
20
25
30
35
40
45
50
Rx location within entity

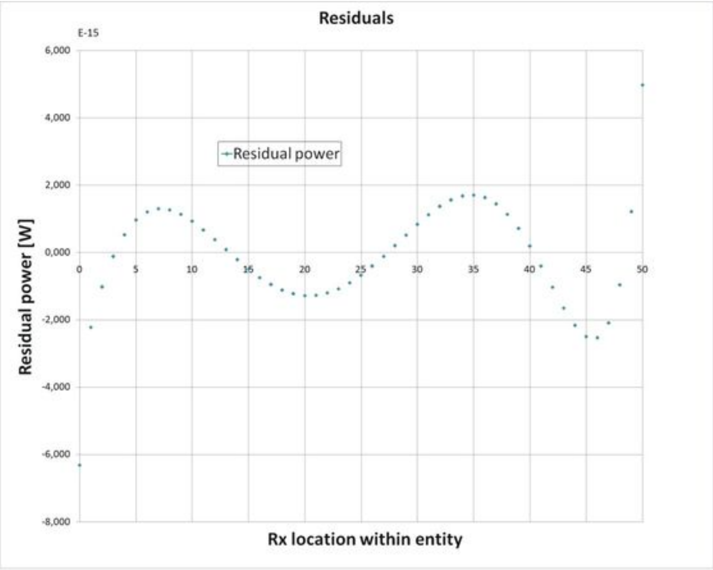
Residuals
E-15
6,000
4,000
2,000
0,000
-2,000
-4,000
-6,000
-8,000
Residual power [W]
Residual power
0
5
10
15
20
25
30
35
40
45
50
Rx location within entity

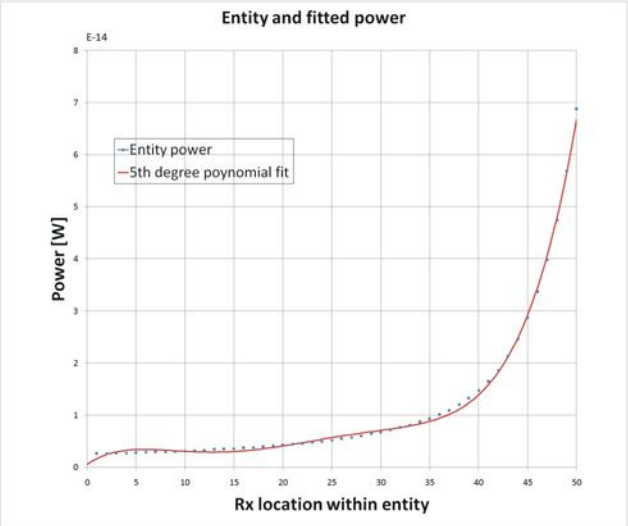
Entity and fitted power
E-14
Entity power
5th degree poynomial fit
Power [W]
Rx location within entity

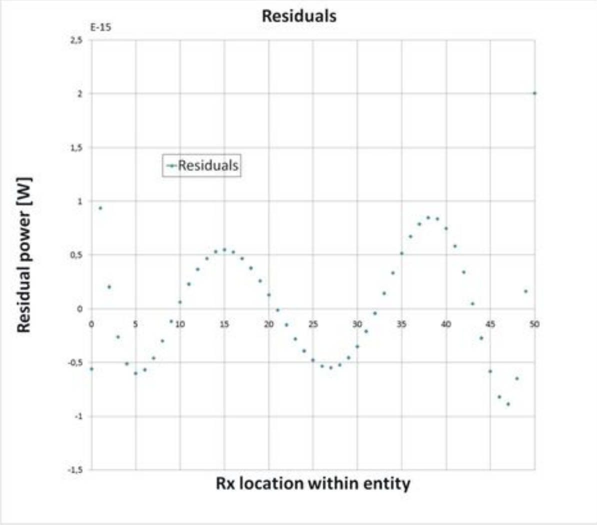
Residuals
E-15
Residuals
Residual power [W]
Rx location within entity